[64] D. W. Colby, Y. Chu, J. P. Cassady et al., "Potent inhibition of huntingtin aggregation and cytotoxicity by a disulfide bond-free single-domain intracellular antibody," *Proceedings of the National Academy of Sciences of the United States of America*, vol. 101, no. 51, pp. 17616–17621, 2004.

[65] A. L. Southwell, A. Khoshnan, D. E. Dunn, C. W. Bugg, D. C. Lo, and P. H. Patterson, "Intrabodies binding the proline-rich domains of mutant Huntingtin increase its turnover and reduce neurotoxicity," *Journal of Neuroscience*, vol. 28, no. 36, pp. 9013–9020, 2008.

[66] A. L. Southwell, J. Ko, and P. H. Patterson, "Intrabody gene therapy ameliorates motor, cognitive, and neuropathological symptoms in multiple mouse models of Huntington's disease," *Journal of Neuroscience*, vol. 29, no. 43, pp. 13589–13602, 2009.

[67] C. E. Wang, H. Zhou, J. R. McGuire et al., "Suppression of neuropil aggregates and neurological symptoms by an intracellular antibody implicates the cytoplasmic toxicity of mutant huntingtin," *Journal of Cell Biology*, vol. 181, no. 5, pp. 803–816, 2008.

[68] E. Dupont, A. Prochiantz, and A. Joliot, "Identification of a signal peptide for unconventional secretion," *Journal of Biological Chemistry*, vol. 282, no. 12, pp. 8994–9000, 2007.

[69] A. M. Bodles, O. M. El-Agnaf, B. Greer, D. J. Guthrie, and G. B. Irvine, "Inhibition of fibril formation and toxicity of a fragment of α-synuclein by an N-methylated peptide analogue," *Neuroscience Letters*, vol. 359, no. 1-2, pp. 89–93, 2004.

[70] C. Soto, E. M. Sigurdsson, L. Morelli, R. A. Kumar, E. M. Castaño, and B. Frangione, "β-sheet breaker peptides inhibit fibrillogenesis in a rat brain model of amyloidosis: implications for Alzheimer's therapy," *Nature Medicine*, vol. 4, no. 7, pp. 822–826, 1998.

Human Molecular Genetics, 2011, Vol. 20, No. 15 **2975–2983**
doi:10.1093/hmg/ddr201
Advance Access published on May 24, 2011

Endoplasmic reticulum stress response in P104L mutant caveolin-3 transgenic mice

Atsushi Kuga[1,2], Yutaka Ohsawa[2], Tadashi Okada[2], Fumio Kanda[1], Motoi Kanagawa[1], Tatsushi Toda[1] and Yoshihide Sunada[2,*]

[1]Division of Neurology/Molecular Brain Science, Kobe University Graduate School of Medicine, 7-5-1 Kusunoki-cho, Kobe, Hyogo 650-0017, Japan and [2]Department of Neurology, Kawasaki Medical School, 577 Matsushima, Kurashiki, Okayama 701-0192, Japan

Received March 28, 2011; Revised March 28, 2011; Accepted April 28, 2011

Mutations in the caveolin-3 gene cause autosomal dominant limb-girdle muscular dystrophy 1C (LGMD1C). However, the precise molecular pathogenesis of caveolin-3-related muscular dystrophy remains uncertain. Here, we demonstrate the effect of gene dosage on the severity of the myopathic phenotype in P104L mutant caveolin-3 (mCav3^{P104L}) transgenic mice, a model of LGMD1C. We analyzed the endoplasmic reticulum (ER) stress response in the transgenic mice and found upregulated transcription of the molecular chaperone, glucose-regulated protein (GRP78). Moreover, signaling downstream of GRP78 in the myofibers was activated toward apoptosis. However, terminal transferase dUTP nick end labeling assays detected a few apoptotic nuclei in transgenic mouse skeletal muscle, probably due to the transcriptional activation of Dad1, an anti-apoptotic factor in the ER. These findings suggest that the ER stress response caused by mCav3^{P104L} plays a role in the pathogenesis of LGMD1C as a toxic gain of function effect.

INTRODUCTION

Caveolae are characterized as flask-shaped invaginations of the plasma membrane (1). Caveolin is a major structural component of caveolae (2) and it also functions as a scaffolding protein to concentrate and regulate many classes of signaling molecules. Distinct genes encode the isoforms, caveolin-1, -2 and -3. Caveolin-3 is specifically expressed in muscle cells (3). Co-expressed caveolins-1 and -2 form hetero-oligomers in non-muscle cells, whereas caveolin-3 forms homo-oligomers in muscle cells. Different mutations in the human caveolin-3 gene have been associated with several muscle diseases that are collectively called caveolinopathies and include limb-girdle muscular dystrophy, distal myopathy and rippling muscle disease (4,5). A mutant caveolin-3 with a single amino acid substitution from proline to leucine at amino acid residue 104 (mCav3^{P104L}) was originally identified from a genetic analysis of autosomal dominant limb-girdle muscular dystrophy 1C (LGMD1C) (6).

Since LGMD1C is inherited as an autosomal dominant trait, mCav3^{P104L} presumably has a dominant-negative effect on the molecular pathogenesis of caveolinopathy. Studies *in vitro* have shown that homo-oligomers of wild-type caveolin-3 translocate to the cell membrane via the endoplasmic reticulum (ER)–Golgi network, whereas mCav3^{P104L} does not target the cell membrane (7). The hetero-oligomers formed between wild-type caveolin-3 and mCav3^{P104L} in the ER–Golgi system are degraded by the ubiquitin–proteasome proteolytic pathway, which might lead to the loss of caveolin-3 in LGMD1C (7,8). Targeted downregulation of caveolin-3 gene in differentiating C2C12 myoblasts can inhibit myotube formation (9). Expression of mCav3^{P104L} can trigger a loss of caveolin-3 during C2C12 cell differentiation (10). These results suggest that the secondary loss of caveolin-3 due to mCav3^{P104L} is associated with the molecular pathology of LGMD1C. However, whether mCav3^{P104L} has a gain of function effect that contributes to the pathogenesis of LGMD1C remains uncertain.

The ER stress response to the accumulation of a mutant protein has recently garnered interest among those investigating the pathogenesis of neurodegenerative disorders. For instance, the cytoplasmic aggregation of alpha-synuclein that is a pathological hallmark of Parkinson's disease is accelerated in a form of familial Parkinson's disease caused by a dominant mutation of the alpha-synuclein gene (11). In addition, several genes responsible for autosomal recessive Parkinson's disease

*To whom correspondence should be addressed. Tel: +81 864621111; Fax: +81 864621199; Email: ysunada@med.kawasaki-m.ac.jp

are involved in the ER-associated ubiquitination system (12). However, the ER stress response has not been intensively studied from the viewpoint of muscular dystrophy. We previously generated and studied mCav3^{P104L} transgenic mice as a model of LGMD1C (13–15). The present study investigates the ER stress response in mCav3^{P104L} transgenic mice as well as a possible gain of function effect of mCav3^{P104L}.

RESULTS

Dose effect of mCav3^{P104L} transgene on the severity of the myopathic phenotype

We previously identified a severe myopathic phenotype in mCav3^{P104L} hemizygous transgenic mice (13). Homozygous mCav3^{P104L} mice were obtained by hemizygous intercrossing and southern blot analysis confirmed the wild-type, hemizygous and homozygous transgenic mouse genotypes (Fig. 1A). Western blot analysis detected less caveolin-3 protein in hemizygous than in homozygous mice (Fig. 1B). We then analyzed the effect of mCav3^{P104L} gene dosages on the myopathic phenotype. Consistent with our previous findings (13), hemizygous mice weighed less than wild-type mice, but the difference did not reach statistical significance. The difference in body weight between homozygous and wild-type mice was statistically confirmed from 4 and 12 weeks of age at all measured points (Fig. 1C). We also found that grip strength significantly differed between the groups from 4 and 12 weeks of age at most measured points (Fig. 1D). Central nucleation or mononuclear infiltration was essentially absent. We measured average areas of myofibers in quadriceps muscles from mice of each genotype (Fig. 1E). Small myofibers were more frequent in the order of homozygous > hemizygous > wild-type mice and non-parametrical statistical analysis confirmed significant differences among the groups (Fig. 1F). The frequency of small myofibers in the gastrocnemius muscle also significantly differed among the genotypes (Supplementary Material, Fig. S1A and B). These data showed that the dose of the mCav3^{P104L} transgene correlated with the severity of the myopathic phenotype.

Residual level of caveolin-3 protein and the myopathic phenotype

The residual amount of caveolin-3 protein in mCav3^{P104L} transgenic mice was <20% of that in wild-type mice (Fig. 1B). To confirm whether other caveolin isoforms counteract the loss of caveolin-3 in muscle cells, we analyzed the expression of caveolin-1 and -2 in mCav3^{P104L} transgenic mice. Messenger RNA levels of caveolin-1 and -2 were increased about 1.5-fold in the skeletal muscle of homozygous mice, whereas no significant change was detectable in hemizygous mice (Fig. 2A and B). Western blotting showed that these changes were consistent at the protein level (Fig. 2C and D). However, immunohistochemistry revealed that upregulated caveolins-1 and -2 were not localized to the sarcolemma, but to the muscle interstitial region containing blood vessels (Fig. 2E). These results indicated that caveolin-1 and -2 upregulation does not compensate for the lack of caveolin-3 function in skeletal muscle. Interestingly, less caveolin-3 protein was detected in hemizygous than in homozygous mice (Fig. 1B). Since the antibodies used for western blotting cannot distinguish between endogenous and mutant caveolin-3 protein, these results suggest that the increased amount of residual mCav3^{P104L} protein in homozygous mice led to more severe myopathy via a toxic gain of function effect.

Localization of mCav3^{P104L} protein and ER stress response

We investigated the subcellular localization of mCav3^{P104L} *in vitro*. Cosmids containing a fluorescent marker for the ER (DsRed-KDEL) or for the Golgi complex (DsRed-Golgi) were cotransfected with wild-type caveolin-3 or mCav3^{P104L} into C2C12 myoblasts. Immunostaining showed surface membrane localization of wild-type caveolin-3, whereas mCAV3^{P104L} did not target the surface membrane and tended to colocalize with the Golgi, but not the ER marker (Fig. 3). The Golgi marker and mCAV3^{P104L} also colocalized in COS7 cells (Supplementary Material, Fig. S2).

We investigated whether mCav3^{P104L} in muscle cells could induce the ER stress response in mCav3^{P104L} transgenic mice by analyzing the expression of genes related to ER stress. Messenger RNA levels of glucose-regulated protein (GRP78), a molecular chaperone in the ER (16), increased 1.5- and 2.5-fold in hemizygous and homozygous mice, respectively, compared with wild-type mice (Fig. 4A and C). Western blotting also confirmed GRP78 induction at the protein level (Fig. 4B and D). Eukaryotic initiation factor 2α (eIF2α) is phosphorylated in response to GRP78 induction under ER stress (17,18). Although the total amount of eIF2α did not significantly change, the amount of phosphorylated eIF2α was increased in transgenic compared with wild-type mice (Fig. 4B and E). We then evaluated the mRNA levels of C/EBP homologous protein (CHOP), which is a pre-apoptotic transcription factor that functions downstream of phosphorylated eIF2α (18,19), and found that they were significantly increased in mCav3^{P104L} transgenic mice (Fig. 4A and C). Overall, these results suggested that mCav3^{P104L} accumulates in the Golgi complex and induces the ER stress response mediated by the molecular chaperone GRP78 and its downstream pathway.

ER stress response toward apoptosis in myofibers from mCav3^{P104L} transgenic mice

We compared the consequences of the mCav3^{P104L}-induced ER stress response using terminal transferase dUTP nick end labeling (TUNEL) assays of quadriceps muscles from mCav3^{P104L} transgenic mice and other mouse models of muscular dystrophy, namely *mdx* and *dy* mice (Fig. 5A). Several TUNEL-positive nuclei of interstitial cells were located outside the myofibers of *mdx* mice and *dy* mice. To distinguish these cells from apoptotic myofibers, we counted the number of myofibers with TUNEL-positive nuclei. Unlike *mdx* mice and *dy* mice, TUNEL-positive nuclei in mCav3^{P104L} transgenic mice were mainly located inside myofibers. Although the average number of TUNEL-positive myofibers was increased in mCav3^{P104L} transgenic mice, the increase was modest compared with the amount in *mdx* mice and *dy* mice (Fig. 5B).

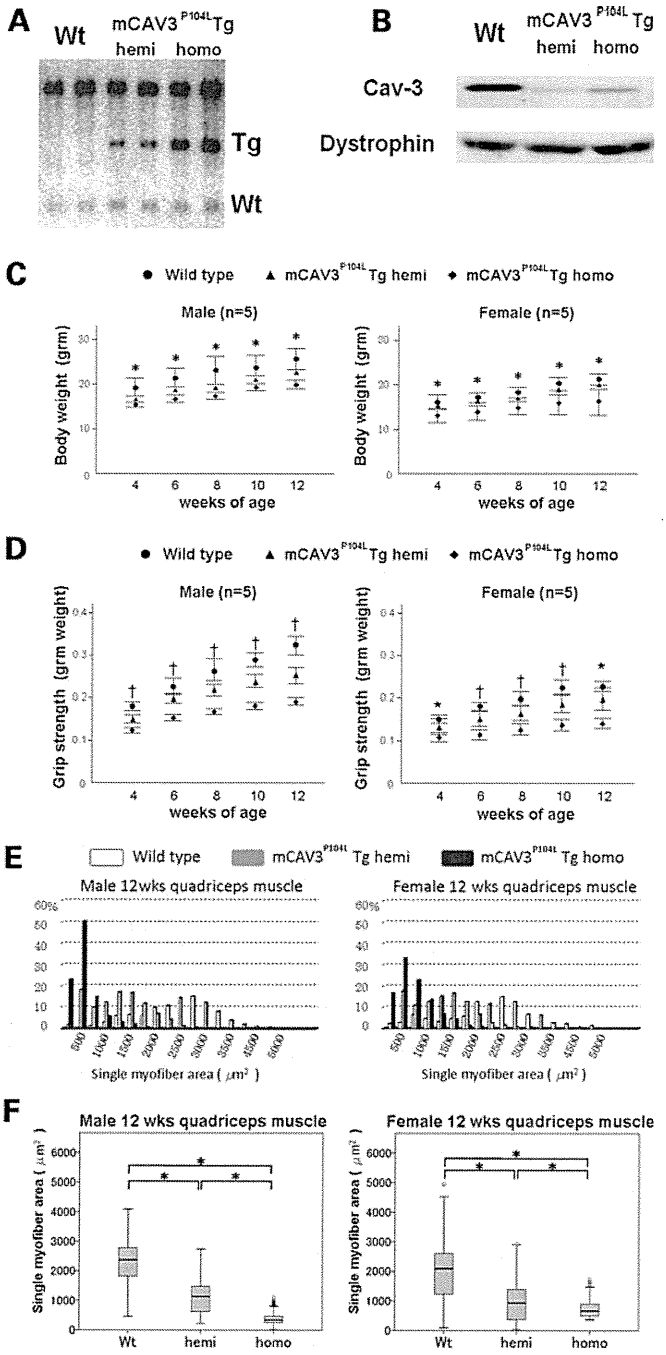

Figure 1. Effect of mCav3^{P104L} transgene dosage on the myopathic phenotype of LGMD1C model mice. (**A**) Genotyping of wild-type, hemizygous and homozygous transgenic mice by Southern blot analysis. A caveolin-3 DNA probe detected both endogenous caveolin-3 gene and mCav3^{P104L} transgene. Left to right, two independent samples of wild-type, hemizygous and homozygous transgenic mice. (**B**) Western blot analysis of caveolin-3 in skeletal muscles of wild-type and mCav3^{P104L} transgenic mice. Levels of caveolin-3 protein obviously decreased in the transgenic mice. Residual caveolin-3 was detected in homozygous mice. Temporal changes in body weight (**C**) and grip strength (**D**) of wild-type and transgenic mice between 4 and 12 weeks of age ($n = 5$ per group). Differences within each group were statistically determined using Scheffe's test. *Significant difference between wild-type and homozygous mice ($P < 0.05$). †Significant difference between each group ($P < 0.05$). Bars indicate standard error. (**E**) Histograms of individual myofiber areas in quadriceps muscle on transverse sections. Values were determined from 1000 myofibers per group. Bar = 100 μm. (**F**) Box plot represents non-parametric statistical analysis of myofiber areas of each group in (E). Significant difference between two groups (Mann–Whitney U test, *$P < 0.005$).

We immunohistochemically analyzed cleaved caspase-3 and cytochrome *c* to further elucidate the ER stress response toward apoptosis in myofibers. Caspase-3 is activated by proteolysis in the signaling cascade toward apoptosis (20). Cleaved caspase-3, which is an active form of caspase-3, is increased in response not only to ER stress but also to

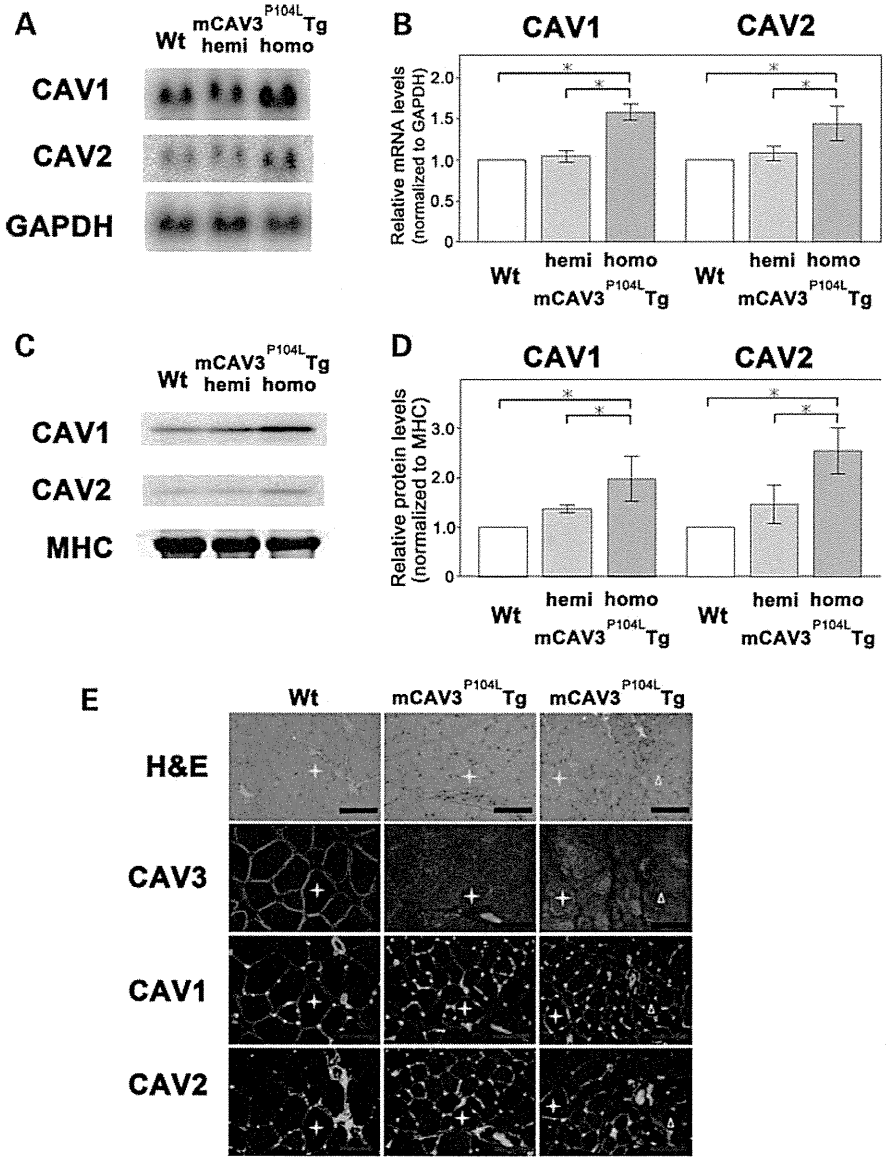

Figure 2. Expression of caveolin isoforms in mCav3^{P104L} transgenic mice. (**A**) Northern blot analysis. Upper panel, caveolin-1; middle panel, caveolin-2; lower panel, GAPDH as control. (**B**) Quantitative analysis of results from (A). (**C**) Western blot analysis. Upper panel, caveolin-1; middle panel, caveolin-2; lower panel, Coomassie blue-stained myosin heavy chain as standard control. (**D**) Quantitative analysis of results from (C). Signal intensity on blots determined from results of five independent experiments. Significant difference ($^*P < 0.05$) determined by Scheffe's test. (**E**) Immunohistochemical analysis of skeletal muscle cryosections from wild-type, hemizygous and homozygous transgenic mice. Crosses and triangles indicate identical myofibers on consecutive sections. H&E, hematoxylin and eosin staining. Caveolin isoforms, green; laminin, red.

apoptotic signals from the mitochondria (20,21). On the other hand, mitochondria specifically release cytochrome *c* into the cytosol under the latter conditions (20,22). Immunoreactivity for cleaved caspase-3 was obvious in the subsarcolemmal area of myofibers in mCav3^{P104L} transgenic mice (Fig. 5A). The average number of cleaved caspase-3 positive myofibers was increased in mCav3^{P104L} transgenic mice and differences between each genotype were significant (Fig. 5C). Cytochrome *c*-positive myofibers were rare in mCav3^{P104L} transgenic mice. Immunostained cleaved caspase-3 covered the entire area of myofibers that were frequently cytochrome *c*-positive in *mdx* and *dy*, but not in mCav3^{P104L} transgenic mice (Fig. 5A).

Apoptotic changes in myofibers were modest in mCav3^{P104L} transgenic mice compared with *mdx* or *dy* mice. We examined the expression of anti-apoptotic molecules from this perspective and found that *Dad1* mRNA was upregulated in mCav3^{P104L} transgenic mice (Fig. 6A and B). Dad1 is a subunit of the oligosaccharyl transferase complex that catalyzes the glycosylation of misfolded proteins to reduce ER stress (23,24). The upregulation of *Dad1* might contribute to the reduction of apoptosis in mCav3^{P104L} transgenic mice.

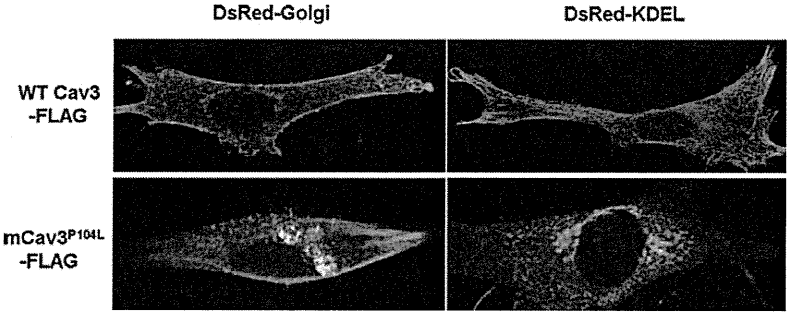

Figure 3. Immunostained C2C12 myoblasts transfected with wild-type or mCav3^{P104L} combined with a fluorescent marker that specifically localizes to ER or Golgi. Wild-type caveolin-3 (upper panels) and mCav3^{P104L} (lower panels) recognized by anti-FLAG tag antibody are shown in green. DsRed-Golgi marker (left panels) and DsRed-ER marker (right panels) recognized by anti-DsRed antibody are shown in red.

DISCUSSION

Mutations of the caveolin-3 gene cause LGMD with an autosomal dominant inheritance (6). Despite numerous studies *in vitro* using the disease-generating P104L mutant caveolin-3 (7–10), details of the molecular pathogenesis underlying LGMD1C have not been fully elucidated. Immunostaining for caveolin-3 at the sarcolemma is obviously lost in patients with LGMD1C (5,6). Galbiati's group proposed a dominant-negative effect of mutant caveolin-3 and demonstrated that it forms unstable aggregates of caveolin-3 hetero-oligomers with wild-type caveolin-3 that are retained in the Golgi complex (7) and that they are likely to be degraded by the ubiquitin–proteasome system (8). These data can explain why caveolin-3 protein levels were reduced in patients with LGMD1C. However, myopathy was notably milder in caveolin-3-null mice (25), but more severe in mCav3^{P104L} transgenic mice (13). Thus, a loss of caveolin-3 caused by the dominant-negative mechanism does not simply account for the severity of the disease in mice. A mechanism other than the reduced expression of caveolin-3 protein might function in the molecular pathogenesis of LGMD1C.

Here, we investigated phenotypic differences between hemizygous and homozygous mCAV3^{P104L} transgenic mice from morphological and molecular aspects. Myofiber hypotrophy and muscular weakness were more prominent in homozygous than in hemizygous mice. These findings indicated that the dosage of the mutant caveolin-3 transgene correlates with the severity of the myopathic phenotype. However, the lower level of residual caveolin-3 protein in hemizygous than in homozygous muscles is curious. This finding suggests that the level of mutant caveolin-3 determines the severity of myopathy through a toxic gain of function effect.

A unique feature of human LGMD1C is subsarcolemmal Golgi accumulation (possibly sarcoplasmic bodies) (5). The present and other studies have demonstrated mCav3^{P104L} accumulation in the Golgi apparatus *in vitro* (7,8,26). Previous pulse-chase experiments revealed that wild-type caveolin forms oligomers of about 400 kDa soon after the protein is synthesized in the ER (27). In addition, the mCav3^{P104L} proteins retained in the Golgi are composed of over 400 kDa high-molecular aggregates, and a proteasomal inhibitor causes such aggregates to accumulate within the ER (8). Together, newly synthesized mutant caveolin-3 protein could rapidly form misfolded aggregates in the ER, thereby inducing the ER stress response. Therefore, we analyzed the ER stress response to investigate a toxic gain of function effect of mCav3^{P104L}.

Indeed, we found that mCAV3^{P104L} induces the ER stress response in a gene-dose-dependent manner. Transcription of the molecular chaperone GRP78 was upregulated in mCav3^{P104L} transgenic mice. Under normal conditions, GRP78 suppresses the ER stress signaling pathway through direct interaction with ER stress transducers, such as PERK (16), which is a serine/threonine kinase that phosphorylates eIF2α (17,18). Misfolded proteins in the ER enlist GRP78 as a molecular chaperone. Once released from GRP78, the ER stress transducers trigger the cascade of gene regulation, known as the unfolded protein response (UPR). Molecular chaperones are commonly activated transcriptionally in the UPR (16). The phosphorylation of eIF2α by PERK is a crucial step in the UPR (17,18). We showed here that these molecular events occur in the skeletal muscle of mCav3^{P104L} transgenic mice, although PERK kinase activity was not directly demonstrated.

We also found that anti-apoptotic Dad1 (23,24) together with pro-apoptotic CHOP (18,19) is gene-dose dependently upregulated in mCAV3^{P104L} transgenic mice. This finding may be consistent with the limited numbers of TUNEL-positive myonuclei and cleaved caspase-3-positive myofibers in mCAV3^{P104L} transgenic mice compared with *mdx* or *dy* mice. Dystrophic changes such as necrotic/regenerating fibers or central nucleation are rarely observed and obvious myofiber hypotrophy is the most prominent feature of mCav3^{P104L} transgenic mice. Transgenic mice weigh less than wild-type mice by 4 weeks of age, which suggests the absence of normal hypertrophic growth or hypoplasia of the skeletal muscle. The most recent findings *in vitro* have revealed that the stable mCav3^{P104L} expression delays myoblast fusion (26). Therefore, the predominant small myofibers might be the result of impaired myotube formation rather than apoptosis. Overall, our results indicate that the apoptotic signaling in response to ER stress is counteracted by anti-apoptotic signaling in myofibers of mCav3^{P104L} transgenic mice, and that its contribution to myopathic change may be modest.

In conclusion, we demonstrated that mutant caveolin-3 dose-dependently induces the ER stress response, which would be a toxic gain of function effect related to the pathophysiology of LGMD1C.

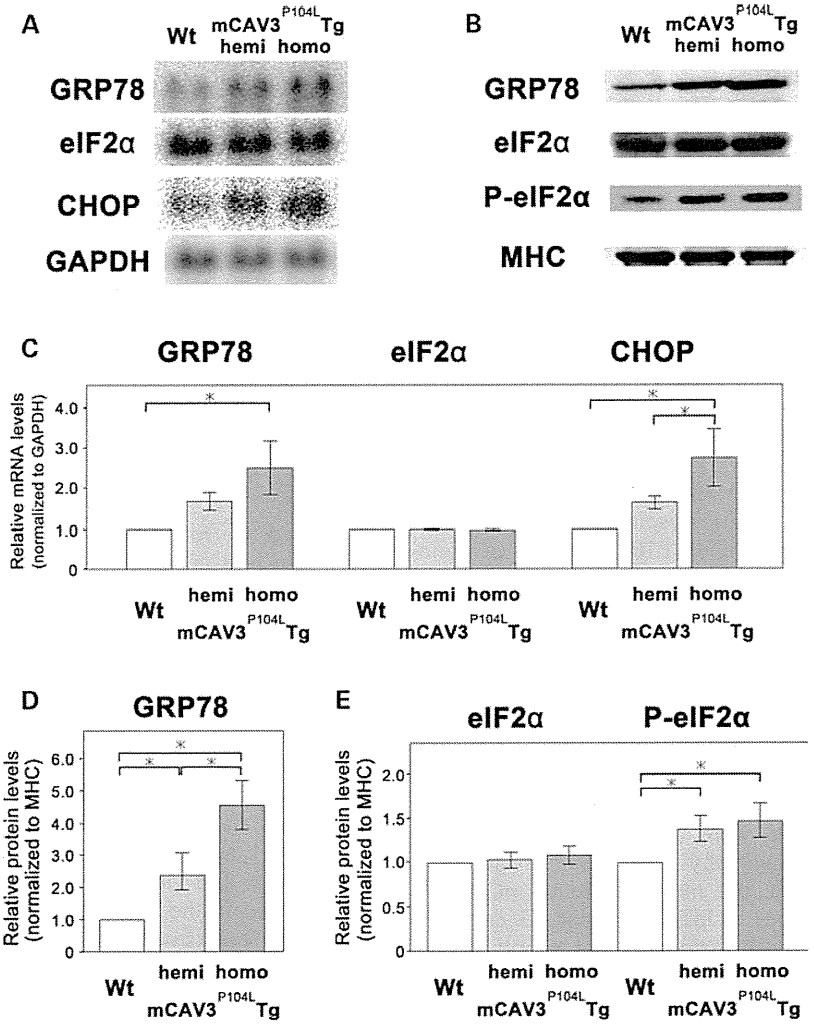

Figure 4. Endoplasmic reticulum stress response in mCav3^{P104L} transgenic mice. (**A**) Northern blot analysis of skeletal muscle from each group. Upper to lower panels, mRNA levels of GRP78, CHOP, eIF2α and GAPDH. (**B**) Western blot analysis of skeletal muscle from each group. Upper to lower panels, protein levels of GRP78, eIF2α and phosphorylated-eIF2α. Control Coomassie blue-stained myosin heavy chain. (**C**) Quantitative analysis of results from (A). (**D**) Quantitative analysis of GRP78 expression based on results from (B). Signal intensity on blots determined from results of five independent experiments. *Significant difference determined by Scheffe's test ($P < 0.05$).

MATERIALS AND METHODS

Animals

Mice were aged about 12 weeks in this study. The construct for the generation of mCav3^{P104L} transgenic mice has been described (13,14). All animal experiments proceeded at the Laboratory Animal Center under the approval of the Animal Research Committee of Kawasaki Medical School.

Muscle morphology and immunohistochemistry

Unfixed distal hindlimb muscles were snap-frozen in liquid nitrogen-cooled isopentane and sectioned transversely (10 μm) at the center of tibialis anterior (or quadriceps) muscle using a cryostat (Leica Microsystems). Sections were post-fixed in cold methanol for 10 min, and then immunostained using the Mouse on Mouse Kit (Vector Laboratories) according to the manufacturer's recommendations. The primary antibodies were as follows: rabbit polyclonal anti-caveolin-1 (BD Transduction Laboratories), mouse monoclonal anti-caveolin-2 (BD Transduction Laboratories), rabbit polyclonal anti-caveolin-3 (Alexis Corporation), rabbit polyclonal anti-cleaved caspase-3 (Cell Signaling Technology), anti cytochrome *c* (eBioscience) and rat monoclonal anti-laminin α2 (Alexis Corporation). Secondary antibodies were conjugated with fluorescein isothiocyanate.

Cell staining

C2C12 and COS7 cells were cultured on coverslips treated with the FuGENE6 transfection reagent (Roche) and then cotransfected with a caveolin-3-FLAG vector or an

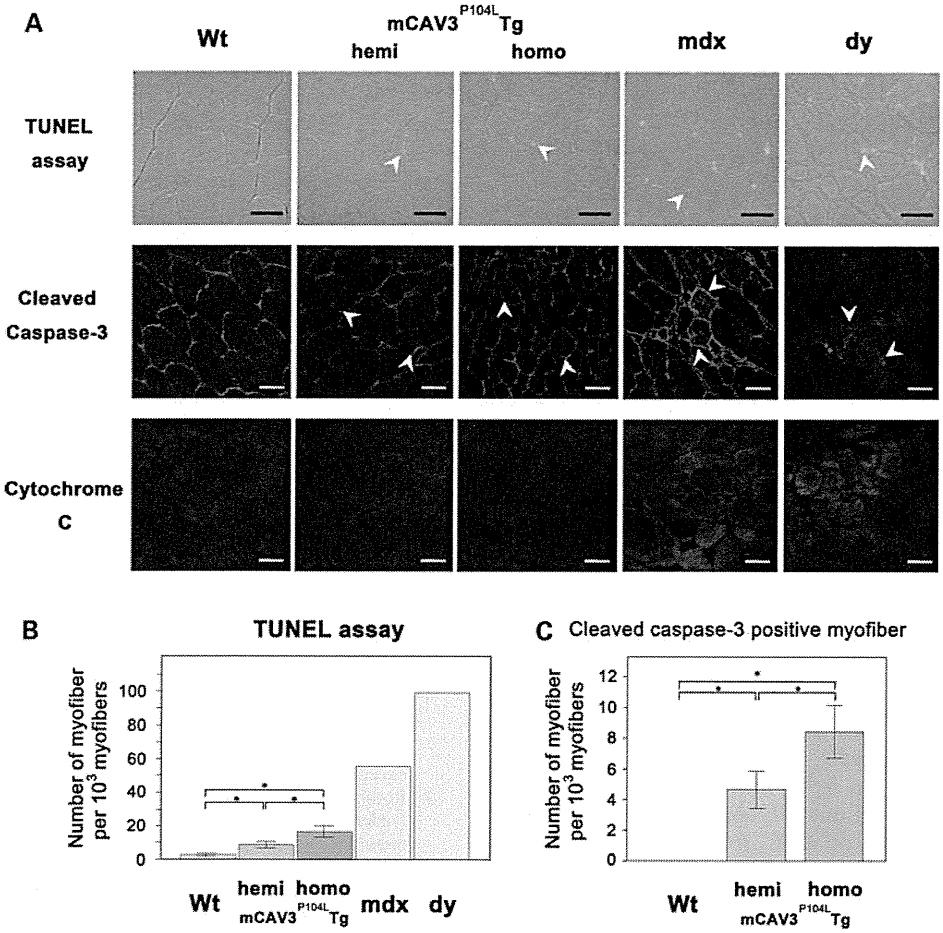

Figure 5. (**A**) (Upper panels) Typical appearance of apoptotic nuclei detected by TUNEL assays in mouse models of muscular dystrophy. Arrowheads indicate TUNEL-positive nuclei inside myofibers. (Middle and lower) Immunohistochemical analysis of skeletal muscle cryosections from mouse models of muscular dystrophy. (Middle panels) Cleaved caspase-3, red; laminin, green; DAPI, blue. Arrowheads indicate myofibers with immunoreactivity for cleaved caspase-3. (Lower panels) Cytochrome *c*, green. Bar = 50 μm (**B**) Numbers of myofibers with TUNEL-positive nuclei calculated per 1000 myofibers from independent samples ($n = 4$ per group of mutant caveolin-3 transgenic mice; positive control *mdx* and *dy* mice; $n = 2$ per group). Significant difference determined by Scheffe's test ($^*P < 0.05$). (**C**) Numbers of myofibers that were immunoreactive for cleaved caspase-3 per 1000 myofibers ($n = 3$ per group of mutant caveolin-3 transgenic mice). Significant difference determined by Scheffe's test ($^*P < 0.05$).

mCav3^{P104L} vector and pDsRed-Golgi (Clontech) or pCS2-DsRed-KDEL (a gift from Dr S. Nishimatsu). Twelve hours later, the cells were fixed in phosphate-buffered saline (PBS) containing 4% paraformaldehyde for 15 min and then permeabilized with PBS containing 0.5% Triton X-100 for 15 min. Non-specific binding was blocked with 3% bovine serum albumin in PBS containing 0.5% Triton X-100 for 1 h at room temperature. Cells were incubated with an anti-FLAG antibody (Sigma) and an anti-DsRed antibody (Clontech) at 4°C, followed by a secondary antibody.

TUNEL assay

Cryosections of quadriceps muscles (10 μm) were fixed with 1% paraformaldehyde in PBS for 10 min at room temperature. The sections were then post-fixed in ethanol:acetic acid (2:1) for 5 min at −20°C, labeled with digoxigenin-conjugated dNTP via the enzymatic activity of terminal deoxynucleotidyl transferase and reacted with anti-digoxigenin fluorescein antibody according to the manufacturer's recommendations (Chemicon). TUNEL-positive nuclei were counted in photographs of 15 sections from each sample.

RT-PCR

We reverse-transcribed cDNA templates from RNAs extracted from C2C12 cells. Genes were amplified using the following respective forward and reverse primers: caveolin-1, 5′-GACTGCCAAGCCTGTTGTAA-3′ and 5′-CAAACTGTG GCCATGCCAG-3′; caveolin-2, 5′-CATAAGGCTAGCTAG AGGCA-3′ and 5′-GGAGAGAACACCTAGACAGC-3′; GRP78, 5′CTTCGAAGGAGAAGACTTCTC-3′ and 5′-CTG TACCTTTGTCTTCAGCTG-3′; eIF2α, 5′-ATCTAATAGC TCCACCCAGG-3′ and 5′-AACAGCTGACATGA AGGAGG-3′; CHOP, 5′-CTGCCTTTCACCTTGGAGAC-3′ and 5′-GCTCGATTTCCTGCTTGAGC-3′; GAPDH, 5′-CGT AGACAAAATGGTGAAGG-3′ and 5′-GTTGTCATGGA TGACCTTGG-3′.

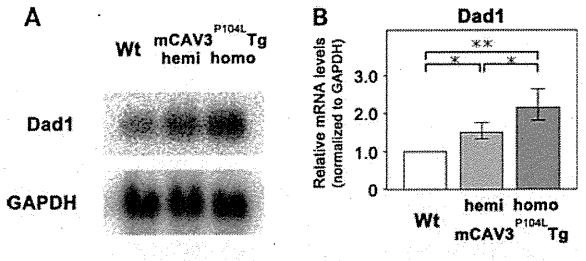

Figure 6. Upregulation of an anti-apoptotic molecule, Dad1, in mCav3^{P104L} transgenic mice. (**A**) Northern blot analysis of Dad1 in skeletal muscle from wild-type, hemizygous and homozygous transgenic mice. (**B**) Quantitative analysis of results from (A). Signal intensity on blots determined from results of five independent experiments. Significant difference determined by Scheffe's test ($^*P < 0.05$).

Northern blot analysis

The RT-PCR products of mouse cDNAs were subcloned into pCRII-TOPO (Invitrogen) and then digested with EcoRI. The digest was separated by agarose gel electrophoresis and extracted using the Rapid Gel Extraction System (Marligen Bioscience). Fragments of DNA were then labeled with [α-^{32}P]-dCTP using the MegaPrime DNA Labeling System (GE Healthcare) and RNAs were extracted from the skeletal muscles of mice in each genotype group. Total RNA (20 μg) was separated on 0.9% agarose gels containing 7% formaldehyde and blotted onto Hybond-N$^+$ (GE Healthcare). Hybridization proceeded at 42°C for 24 h, and then bands were visualized by autoradiography using Fuji Imaging Plates (Fujifilm). All northern blot experiments were repeated at least three times using different sets of samples.

Western blot analysis

Mouse skeletal muscles were homogenized in 10 volumes (w/v) of a buffer comprising 50 mM Tris–HCl (pH 7.4), 100 mM NaCl, 1 mM EDTA, 5 mM β-mercaptoethanol, 0.1 mM PMSF and 1 mM benzamidine. Crude muscle homogenates were separated by SDS-PAGE (3–20% linear acrylamide gradient) and transferred to polyvinylidene difluoride membranes. Antibodies were purchased from the indicated sources: goat polyclonal anti-GRP78 (Santa Cruz Biotechnology), mouse monoclonal anti-eIF2α (Abcam), rabbit polyclonal anti-Ser51 phosphorylated eIF2α (Abcam), rabbit polyclonal anti-caveolin-1 (BD Transduction Laboratories), mouse monoclonal anti-caveolin-2 (BD Transduction Laboratories) and rabbit polyclonal anti-caveolin-3 (Alexis Corporation). All western blot experiments were repeated at least five times, with different sets of samples. Immunoblot band intensities were standardized with Coomassie blue staining of myosin heavy chain in each sample and analyzed using Multi Gauge version 2.2 software (Fujifilm).

SUPPLEMENTARY MATERIAL

Supplementary Material is available at *HMG* online.

ACKNOWLEDGEMENTS

We thank M. Fujino (postgraduate student, Kawasaki Welfare School), A. Mimura, N. Oka and K. Yamane (Kawasaki Medical School), as well as N. Naoe and T. Kenmotsu (Department of Neurology, Kawasaki Medical School) for excellent technical assistance.

Conflict of Interest statement. None declared.

FUNDING

This study was supported by JSPS KAKENHI 20591013 and 21591101, a research grant for Nervous and Mental Disorders from the Ministry of Health, Labour and Welfare of Japan (20B-13), by grants for Research on Psychiatric and Neurological Diseases and Mental Health from the Ministry of Health, Labour and Welfare of Japan (H20-016, H20-018) and by research project grants from the Kawasaki Medical School (20-604, 21-602 and 22-T1).

REFERENCES

1. Richter, T., Floetenmeyer, M., Ferguson, C., Galea, J., Goh, J., Lindsay, M.R., Morgan, G.P., Marsh, B.J. and Parton, R.G. (2008) High-resolution 3D quantitative analysis of caveolar ultrastructure and caveola-cytoskeleton interactions. *Traffic*, **9**, 893–909.
2. Rothberg, K.G., Heuser, J.E., Donzell, W.C., Ying, Y., Glenney, J.R. and Anderson, R.G.W. (1992) Caveolin, a protein component of caveolae membrane coats. *Cell*, **68**, 673–682.
3. Song, K.S., Scherer, P.E., Tang, Z., Okamoto, T., Li, S., Chafel, M., Chu, C., Kohtz, D.S. and Lisanti, M.P. (1996) Expression of caveolin-3 in skeletal, cardiac, and smooth muscle cells. *J. Biol. Chem.*, **271**, 15160–15165.
4. Woodman, S.E., Sotgia, F., Galbiati, F., Minetti, C. and Lisanti, M.P. (2004) Caveolinopathies: mutations in caveolin-3 cause four distinct autosomal dominant muscle diseases. *Neurology*, **62**, 538–543.
5. Fulizio, L., Nascimbeni, A.C., Fanin, M., Piluso, G., Politano, L., Nigro, V. and Angelini, C. (2005) Molecular and muscle pathology in a series of caveolinopathy patients. *Hum. Mutat.*, **25**, 82–89.
6. Minetti, C., Sotgia, F., Bruno, C., Scartezzini, P., Broda, P., Bado, M., Masetti, E., Mazzocco, M., Egeo, A., Donati, M.A. *et al.* (1998) Mutations in the caveolin-3 gene cause autosomal dominant limb-girdle muscular dystrophy. *Nat. Genet.*, **18**, 365–368.
7. Galbiati, F., Volonté, D., Minetti, C., Chu, J.B. and Lisanti, M.P. (1999) Phenotypic behavior of caveolin-3 mutations that cause autosomal dominant limb girdle muscular dystrophy (LGMD-1C). *J. Biol. Chem.*, **274**, 25632–25641.
8. Galbiati, F., Volonté, D., Minetti, C., Bregman, D.B. and Lisanti, M.P. (2000) Limb-girdle muscular dystrophy (LGMD-1C) mutants of caveolin-3 undergo ubiquitination and proteasomal degradation. *J. Biol. Chem.*, **275**, 37702–37711.
9. Galbiati, F., Volonté, D., Engelman, J.A., Scherer, P.E. and Lisanti, M.P. (1999) Targeted down-regulation of caveolin-3 is sufficient to inhibit myotube formation in differentiating C2C12 myoblasts. *J. Biol. Chem.*, **274**, 30315–30321.
10. Fanzani, A., Stoppani, E., Gualandi, L., Giuliani, R., Galbiati, F., Rossi, S., Fra, A., Preti, A. and Marchesini, S. (2007) Phenotypic behavior of C2C12 myoblasts upon expression of the dystrophy-related caveolin-3 P104L and TFT mutants. *FEBS Lett.*, **581**, 5099–5104.
11. Conway, K.A., Harper, J.D. and Lansbury, P.T. (1998) Accelerated in vitro fibril formation by a mutant alpha-synuclein linked to early-onset Parkinson disease. *Nat. Med.*, **4**, 1318–1320.
12. Xiong, H., Wang, D., Chen, L., Choo, Y.S., Ma, H., Tang, C., Xia, K., Jiang, W., Ronai, Z., Zhuang, X. *et al.* (2009) Parkin, PINK1, and DJ-1 form a ubiquitin E3 ligase complex promoting unfolded protein degradation. *J. Clin. Invest.*, **119**, 650–660.

13. Sunada, Y., Ohi, H., Hase, A., Ohi, H., Hosono, T., Arata, S., Higuchi, S., Matsumura, K. and Shimizu, T. (2001) Transgenic mice expressing mutant caveolin-3 show severe myopathy associated with increased nNOS activity. *Hum. Mol. Genet.*, **10**, 173–178.
14. Ohsawa, Y., Toko, H., Katsura, M., Morimoto, K., Yamada, H., Ichikawa, Y., Murakami, T., Ohkuma, S., Komuro, I. and Sunada, Y. (2004) Overexpression of P104L mutant caveolin-3 in mice develops hypertrophic cardiomyopathy with enhanced contractility in association with increased endothelial nitric oxide synthase activity. *Hum. Mol. Genet.*, **13**, 151–157.
15. Ohsawa, Y., Hagiwara, H., Nakatani, M., Yasue, A., Moriyama, K., Murakami, T., Tsuchida, K., Noji, S. and Sunada, Y. (2006) Muscular atrophy of caveolin-3-deficient mice is rescued by myostatin inhibition. *J. Clin. Invest.*, **116**, 2924–2934.
16. Ni, M. and Lee, A.S. (2007) ER chaperones in mammalian development and human diseases. *FEBS Lett.*, **581**, 3641–3651.
17. Harding, H.P., Zhang, Y., Bertolotti, A., Zeng, H. and Ron, D. (2000) PERK is essential for translational regulation and cell survival during the unfolded protein response. *Mol. Cell*, **5**, 897–904.
18. Harding, H.P., Novoa, I., Zhang, Y., Zeng, H., Wek, R., Schapira, M. and Ron, D. (2000) Regulated translation initiation controls stress-induced gene expression in mammalian cells. *Mol. Cell*, **6**, 1099–1108.
19. Oyadomari, S. and Mori, M. (2004) Roles of CHOP/GADD153 in endoplasmic reticulum stress. *Cell Death Differ.*, **11**, 381–389.
20. Li, P., Nijhawan, D., Budihardjo, I., Srinivasula, S.M., Ahmad, M., Alnemri, E.S. and Wang, X. (1997) Cytochrome c and dATP-dependent formation of Apaf-1/caspase-9 complex initiates an apoptotic protease complex. *Cell*, **91**, 479–489.
21. Morishima, N., Nakanishi, K., Takenouchi, H., Shibata, T. and Yasuhiko, Y. (2002) An endoplasmic reticulum stress-specific caspase cascade in apoptosis. *J. Biol. Chem.*, **277**, 34287–34294.
22. Kluck, R.M., Bossy-Wetzel, E., Green, D.R. and Newmeyer, D.D. (1997) The release of cytochrome c from mitochondria. *Science*, **275**, 1132–1136.
23. Kelleher, D.J. and Gilmore, R. (1997) DAD1, the defender against apoptotic cell death, is a subunit of the mammalian oligosaccharyltransferase. *Proc. Natl. Acad. Sci. USA*, **94**, 4994–4999.
24. Kelleher, D.J. and Gilmore, R. (2006) An evolving view of the eukaryotic oligosaccharyltransferase. *Glycobiology*, **16**, 47R–62R.
25. Hagiwara, Y., Sasaoka, T., Araishi, K., Imamura, M., Yorifuji, H., Nonaka, I., Ozawa, E. and Kikuchi, T. (2000) Caveolin-3 deficiency causes muscle degeneration in mice. *Hum. Mol. Genet.*, **9**, 3047–3054.
26. Stoppani, E., Rossi, S., Meacci, E., Penna, F., Costelli, P., Bellucci, A., Faggi, F., Maiolo, D., Monti, E. and Fanzani, A. (2011) Point mutated caveolin-3 form (P104L) impairs myoblast differentiation via Akt and p38 signalling reduction, leading to an immature cell signature. *Biochim. Biophys. Acta*, **1812**, 468–479.
27. Monier, S., Parton, R.G., Vogel, F., Behlke, J., Henske, A. and Kurzchalia, T.V. (1995) VIP21-caveolin, a membrane protein constituent of the caveolar coat, oligomerizes in vivo and in vitro. *Mol. Biol. Cell*, **6**, 911–927.

THE JOURNAL OF BIOLOGICAL CHEMISTRY VOL. 287, NO. 12, pp. 9560–9567, March 16, 2012

Absence of Post-phosphoryl Modification in Dystroglycanopathy Mouse Models and Wild-type Tissues Expressing Non-laminin Binding Form of α-Dystroglycan*[S]

Received for publication, June 14, 2011, and in revised form, January 13, 2012 Published, JBC Papers in Press, January 23, 2012, DOI 10.1074/jbc.M111.271767

Atsushi Kuga[‡], Motoi Kanagawa[‡], Atsushi Sudo[‡], Yiumo Michael Chan[§], Michiko Tajiri[¶], Hiroshi Manya[‖], Yamato Kikkawa[**], Motoyoshi Nomizu[**], Kazuhiro Kobayashi[‡], Tamao Endo[‖], Qi L. Lu[§], Yoshinao Wada[¶], and Tatsushi Toda[‡1]

From the [‡]Division of Neurology/Molecular Brain Science, Kobe University Graduate School of Medicine, Kobe 650-0017, Japan, the [§]McColl-Lockwood Laboratory for Muscular Dystrophy Research, Neuromuscular/ALS Center, Carolinas Medical Center, Charlotte, North Carolina 28231, the [¶]Department of Molecular Medicine, Osaka Medical Center and Research Institute for Maternal and Child Health, Osaka 594-1101, Japan, [‖]Molecular Glycobiology, Tokyo Metropolitan Institute of Gerontology, Tokyo 173-0015, Japan, and the [**]Laboratory of Clinical Biochemistry, School of Pharmacy, Tokyo University of Pharmacy and Life Sciences, Tokyo 192-0392, Japan

Background: The biosynthetic pathway for the ligand-binding moiety of α-dystroglycan, defects in which cause dystroglycanopathy, remains unclear.
Results: The phosphodiester-linked moiety on *O*-mannose is absent in dystroglycanopathy models and in wild-type lung and testis.
Conclusion: Post-phosphoryl modification is a key determinant of the functional expression of α-dystroglycan as a laminin receptor.
Significance: This work expands our understanding of the molecular mechanism of a unique post-translational modification.

α-Dystroglycan (α-DG) is a membrane-associated glycoprotein that interacts with several extracellular matrix proteins, including laminin and agrin. Aberrant glycosylation of α-DG disrupts its interaction with ligands and causes a certain type of muscular dystrophy commonly referred to as dystroglycanopathy. It has been reported that a unique *O*-mannosyl tetrasaccharide (Neu5Ac-α2,3-Gal-β1,4-GlcNAc-β1,2-Man) and a phosphodiester-linked modification on *O*-mannose play important roles in the laminin binding activity of α-DG. In this study, we use several dystroglycanopathy mouse models to demonstrate that, in addition to fukutin and LARGE, FKRP (fukutin-related protein) is also involved in the post-phosphoryl modification of *O*-mannose on α-DG. Furthermore, we have found that the glycosylation status of α-DG in lung and testis is minimally affected by defects in *fukutin*, *LARGE*, or *FKRP*. α-DG prepared from wild-type lung- or testis-derived cells lacks the post-phosphoryl moiety and shows little laminin-binding activity. These results show that FKRP is involved in post-phosphoryl modification rather than in *O*-mannosyl tetrasaccharide synthesis. Our data also demonstrate that post-phosphoryl modification not only plays critical roles in the pathogenesis of dystroglycanopathy but also is a key determinant of α-DG functional expression as a laminin receptor in normal tissues and cells.

Dystroglycan (DG),[2] a cell surface receptor for several extracellular matrix proteins, plays important roles in various tissues (1). DG consists of a heavily glycosylated extracellular α subunit (α-DG) and a transmembrane β subunit (β-DG). α-DG and β-DG are encoded by a single gene and post-translationally cleaved to generate the two subunits (2). α-DG binds to extracellular proteins such as laminin, agrin, perlecan, neurexin, and pikachurin (2–7). β-DG anchors α-DG at the cell surface and binds intracellularly to dystrophin, which in turn binds to the actin cytoskeleton. Thus, α/β-DG functions as a molecular axis, connecting the extracellular matrix with the cytoskeleton across the plasma membrane (1).

O-Glycosylation of α-DG is necessary for its interaction with ligands, and genetic disruption of the glycosylation pathway for DG is associated with a group of muscular dystrophies known as "dystroglycanopathy" (8–10). Six genes (*POMT1*, *POMT2*, *POMGnT1*, *fukutin*, *FKRP*, and *LARGE*) have been identified as causative genes for dystroglycanopathy. A common biochemical characteristic of these disorders is abnormal glycosylation and reduced laminin-binding activity of α-DG; however, the precise glycan structure required for α-DG ligand binding is not completely determined. Two unique *O*-mannosyl modifications have been identified in α-DG: an *O*-mannosyl tetrasaccharide (Neu5Ac-α2,3-Gal-β1,4-GlcNAc-β1,2-Man) (11), and

* This work was supported by Ministry of Health, Labor, and Welfare of Japan Intramural Research Grant (23B-5) for Neurological and Mental Disorders and The Research on Psychiatric and Neurological Diseases and Mental Health H20-016 (to T. T.), Grant-in-aid for Scientific Research (A) 23249049 (to T. T.) and a Grant-in-aid for Young Scientists (B) 21790318 (to M. K.) from the Ministry of Education, Culture, Sports, Science, and Technology of Japan, and the Takeda Science Foundation (to M. K.).
[S] This article contains supplemental Fig. 1.
[1] To whom correspondence should be addressed: 7-5-1 Kusunoki-chou Chuo-ku, Kobe 650-0017, Japan. Tel.: 81-78-382-6287; Fax: 81-78-382-6288; E-mail : toda@med.kobe-u.ac.jp.

[2] The abbreviations used are: DG, dystroglycan; IMAC, immobilized metal affinity chromatography; MW, molecular weight; HFaq, aqueous hydrofluoric acid.

a phosphodiester-linked branch structure present at the C6 hydroxyl residue of *O*-mannose (12). The *O*-mannosyl tetrasaccharide was first identified on peripheral nerve α-DG (11). The initial mannose transferred to Ser/Thr residues on the α-DG polypeptide backbone is catalyzed by the POMT1/POMT2 complex (13). Mutations in *POMT1* and *POMT2* were originally identified as causative for Walker-Warburg syndrome (14, 15). *POMGnT1*, established as a causative gene for muscle-eye-brain disease, encodes a glycosyltransferase that transfers GlcNAc to *O*-mannose on α-DG (16). In these disorders, α-DG lacks laminin-binding activity (17); therefore, the tetrasaccharide plays an important role in the post-translational maturation of α-DG as a laminin receptor. On the other hand, recent studies have suggested that the Neu5Ac-α2,3-Gal-β1,4-GlcNAc branch on *O*-mannose *per se* is not likely the laminin-binding glycan of α-DG (12, 18).

fukutin was originally identified as the causative gene for Fukuyama-type congenital muscular dystrophy (19), and *FKRP* was identified as the causative gene for both MDC1C (congenital muscular dystrophy type 1C) (20) and LGMD2I (limb-girdle muscular dystrophy type 2I) (21). The precise function of fukutin and FKRP is still uncertain. Mutation of *LARGE* causes muscular dystrophy in the spontaneous *Large*^{myd} mouse model (22) and in human congenital muscular dystrophy type 1D (23). Recently, a phosphodiester-linked modification on an *O*-mannose was identified (12). It was shown that α-DG in *fukutin*-mutated Fukuyama-type congenital muscular dystrophy and *Large*^{myd} muscle cells exhibits defective post-phosphoryl modification on the *O*-mannose, suggesting that this phosphorylated branch serves as the laminin-binding moiety. To explore the role of phosphorylated *O*-mannose in functional α-DG ligand-binding and in other forms of dystroglycanopathy, we have investigated α-DG glycosylation in several dystroglycanopathy mouse models.

EXPERIMENTAL PROCEDURES

Cell Culture—TM3 and CHL cell lines were purchased from European collection of cell cultures and the RIKEN BioResource Center, respectively. TM3 cells were cultured in Ham's F12/DMEM (1:1) containing 5% horse serum and 2.5% fetal bovine serum. CHL cells were cultured in DMEM containing 10% fetal bovine serum. Expression vectors for LARGE were constructed by cloning human *LARGE* with a V5 tag into pcDNA vectors (24). Transfection was carried out using Lipofectamine 2000 (Invitrogen) for CHL and TM3 cells according to the manufacturer's instructions. Transfected cells were grown at 37 °C and harvested at 48 h after transfection. The transfected cells were solubilized in TBS with 1% Triton X-100. Samples were centrifuged at 15,000 rpm for 10 min at 4 °C. Supernatants were collected, and protein concentrations were measured by Lowry methods, using BSA as a standard.

Animals—*Large*^{myd} mice were obtained from The Jackson Laboratory. Generation of FKRP-neo-P448L knock-in mice, Hp/− mice, and *POMGnT1*-deficient mice has been described previously (25–27). Mice were maintained in accordance with the animal care guidelines of Kobe University. All animal studies using FKRP-neo-P448L knock-in mice were approved by the Institutional Animal Care and Use Committee of the Carolinas Medical Center.

Protein Enrichment—Frozen tissue samples were solubilized in TBS (pH 7.4) with 1% Triton X-100. The solubilized materials were incubated with wheat germ agglutinin beads, and the DG-enriched fraction was then eluted with 0.3 M *N*-acetyl-D-glucosamine in TBS containing 0.1% Triton X-100. For the immobilized metal affinity chromatography (IMAC)-binding assay, aqueous hydrofluoric acid (HFaq) treatment, and deglycosylation assay, the DG-enriched fractions were diluted in 0.25% CHAPS/water (w/v) and then desalted and concentrated using Amicon-ultra filters (Millipore).

IMAC-binding Assay—Samples were diluted in a solution containing 250 mM acetic acid, 30% acetonitrile, and 0.15% CHAPS and incubated with PHOS-Select iron affinity gel (Sigma) at room temperature for 0.5 h. Bound materials were directly eluted with SDS-loading buffer. Equal ratios of the void and the bound samples were used for Western blot analysis.

HFaq Treatment—Samples were incubated with 48% aqueous hydrofluoric acid (Wako) on ice for 12 h. Control samples were incubated with water instead of hydrofluoric acid. After removal of the reagents under a stream of nitrogen gas, residues were dissolved with SDS-loading buffer for Western blot analysis.

Deglycosylation Assay—Glycopeptidase F (peptide-*N*-glycosidase; Wako), α-2 (3, 6, 8, 9) neuraminidase (Calbiochem), β1–4 galactosidase (New England Biolabs), β-*N*-acetyl-hexosaminidase (Seikagaku Corp.), and *O*-glycosidase (Roche Applied Science) were used according to the manufacturer's protocol.

Antibodies—Antibodies used for Western blotting were mouse monoclonal antibody IIH6 against glycosylated α-DG (Millipore) and goat polyclonal antibody against the C-terminal domain of the α-DG polypeptide (AP-074G-C) (26).

Laminin and Agrin Overlay Assays—Recombinant mouse laminin LG4–5 domains of laminin α1 and laminin α2 chains fused to Fc tags were recovered from the cell culture media using protein A beads (28). Recombinant agrin was purchased from R&D Systems. Laminin and agrin overlay assays were performed as described previously (26).

RT-PCR Analysis—Total RNA was isolated from wild-type mouse testis and TM3 cells using the RNeasy Plus mini kit (Qiagen) and converted to cDNA using Superscript III reverse transcriptase (Invitrogen). The forward and reverse primers used in gene amplification were as follows: *Large* (5′-TCAATCTTCTGCGAAACGTG-3′ and 5′-TCCAACATTGACAGCAGCTC-3′), *POMT1* (5′-CGGGTCTCTTGTTCCTGTG-3′ and 5′-AGTGACTGAGCACGCGCATA-3′), *POMT2* (5′-CGGAACCTGCACAGTCACTA-3′ and 5′-AATCCGCCAGAAGTCATTTG-3′), *POMGnT1* (5′-CCAAGGGGTATCTCCACAGA-3′ and 5′-GGTCCTCTTCCAGAACCACA-3′), *fukutin* (5′-CGCACTGCAGTATCACCTGT-3′ and 5′-AAGTGGATGGCATGAGTGGT-3′), *FKRP* (5′-CTTCTGTCCCGCTTCAGTTC-3′ and 5′-AACCAGAGAGAGCCCAGTCA-3′), *β3GnT1* (5′-TTCAATCGAATCAGCCAGGTA-3′ and 5′-TCCTCAATTCTCCATCATCCA-3′), GAPDH (5′-CGTAGACAAAATGGTGAAGG-3′ and 5′-GTTGTCATGGAT-

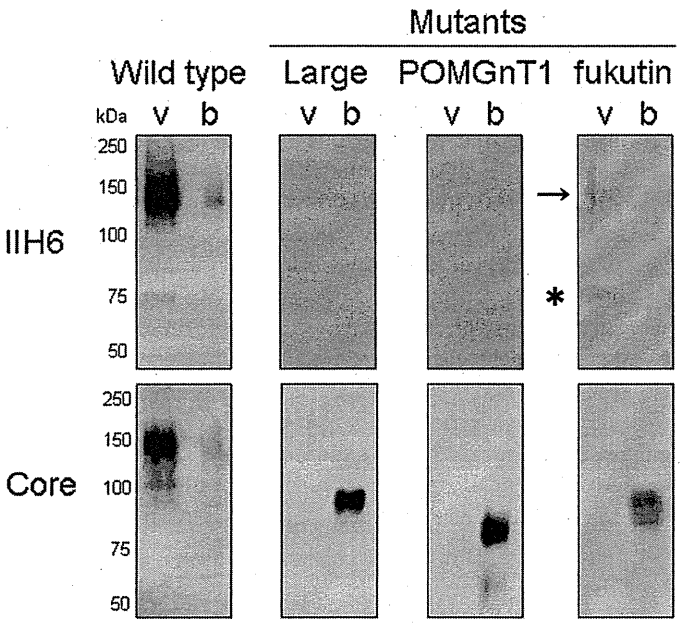

FIGURE 1. **Defects of post-phosphoryl modification in the dystroglycanopathy models.** α-DG-enriched samples from skeletal muscle of wild-type, *Large*^{myd}, *POMGnT1*-deficient, and *fukutin*-deficient Hp/− mice were subjected to IMAC beads. The void (*v*) and bound (*b*) fractions were collected. An *arrow* indicates the IIH6-positive intact α-DG in the Hp/− mice. An *asterisk* indicates a background signal that is not specific for IIH6 antibody.

GACCTTGG-3′), and *DAG1* (5′-ACCAAAGCACCCATCAC-CAG-3′ and 5′-GTTCCCACCCAGGCATCTAC-3′).

RESULTS

Defects of Post-phosphoryl Modification in FKRP-deficient Mice—To examine whether dystroglycanopathy models share a common defect in the post-phosphoryl modification of α-DG, we performed an IMAC bead-binding assay. IMAC beads bind to monoester-linked, but not diester-linked, phosphorylated compounds, and it has been shown that α-DG with defects in post-phosphoryl modification binds to IMAC beads (12). First, we used *Large*^{myd} mice (22), genetically engineered *POMGnT1* knock-out mice (27), and transgenic Hp/− knock-in mice carrying the retrotransposal insertion in *fukutin* (26). α-DG in skeletal muscle tissues from these mutant mice was not properly glycosylated, as indicated by the loss of reactivity against the monoclonal antibody IIH6 (Fig. 1, *upper panel*). The hypoglycosylated α-DG has a lower molecular weight (MW) that can only be detected by the DG core antibody (Fig. 1, *lower panel*). IIH6 antibody reacts with the laminin-binding glycans present in α-DG (17). Hypoglycosylated α-DG was captured by the IMAC beads, indicating that the monoester-linked phosphate residues do not undergo further modification. A small portion of α-DG with a MW of 150,000 in the Hp/− mice (Fig. 1, *arrow*) did not bind to the IMAC beads and showed reactivity against the IIH6 antibody, which might be due to the residual activity of fukutin in the Hp/− mice (26). These data support the observations made in muscle-eye-brain disease and Fukuyama-type congenital muscular dystrophy patients' cells and skeletal muscle biopsies (12).

We next examined whether FKRP is also involved in the post-phosphoryl modification of α-DG. Consistent with previous observations, α-DG from the skeletal muscle of homozygous FKRP-neo-P448L knock-in mice (FKRP-P448L mice) was aberrantly glycosylated, as indicated by the loss of IIH6 reactivity (25). The hypoglycosylated α-DG, showing a lower MW of 90,000 compared with wild-type α-DG at 150,000, bound to the IMAC beads (Fig. 2*A*, *lower panel*). In brain tissue, IIH6-positive α-DG shows a MW of 100,000, whereas hypoglycosylated α-DG shows a MW of 70,000. As was the case in skeletal muscle, hypoglycosylated α-DG from the homozygous mouse bound to IMAC beads (Fig. 2*A*). It has been reported that treatment with cold HFaq cleaves the phosphodiester linker in α-DG (12). After HFaq treatment, the MW of α-DG was reduced to ~90,000, and α-DG lost IIH6-reactivity (Fig. 2*B*, *left panel*). In contrast to the mature α-DG from heterozygous controls, the hypoglycosylated α-DG from homozygous FKRP-P448L muscle showed almost no change in MW after the HFaq treatment (Fig. 2*B*, *right panel*). Treatment with several mixtures of glycosidase predicted to remove *N*-glycan, mucin type *O*-glycan, and the trisaccharide at the non-reducing end of the Neu5Ac-α2,3-Gal-β1,4-GlcNAc-β1,2-Man glycan (12, 18) generated stepwise decreases in the MW of α-DG through multi-step digestions (Fig. 2*C*). These results indicate for the first time that FKRP is involved in the post-phosphoryl modification of α-DG rather than in the synthesis of the Neu5Ac-α2,3-Gal-β1,4-GlcNAc-β1,2-Man glycan. This concept is supported by the previous observation that neither POMT1/2 nor POMGnT1 activity was reduced in lymphoblast cells from patients with *FKRP* mutations (29). Overall, our results establish and confirm that a defect in post-phosphoryl modification on *O*-mannose is a common biochemical characteristic in dystroglycanopathy caused by mutations in *LARGE*, *POMGnT1*, *fukutin*, and *FKRP*.

Post-phosphoryl Moiety of α-dystroglycan Is Absent in Lung and Testis—We have demonstrated that disruption of *Large*, *fukutin*, or *FKRP* decreases the MW of α-DG in skeletal muscle and brain due to the lack of post-phosphoryl modification. It is known that the MW of α-DG and its reactivity to the monoclonal antibody IIH6 vary among different tissues (1, 30). We hypothesized that the low MW of α-DG in some tissues may result from the lack of post-phosphoryl modification and/or the Neu5Ac-α2,3-Gal-β1,4-GlcNAc-β1,2-Man glycan. Several tissues from dystroglycanopathy model mice were therefore investigated. We found that the decreases in the MW of α-DG were relatively minor in lung and very scarce in testis from FKRP-P448L mice and Hp/− mice when compared with litter controls (Fig. 3*A*). Minor changes in α-DG MW in the lung and testis of *Large*-deficient mice have been also observed elsewhere (30), supporting our findings. On the other hand, α-DG in lung and testis from *POMGnT1*-deficient mice clearly shows a lower MW compared with litter heterozygous controls and other mutant mouse strains (Fig. 3*B*). These results suggested that the GlcNAc-β1,2 branch on *O*-mannose is present in wild-type α-DG in lung and testis, but post-phosphoryl modification is absent.

We examined these tissues in wild-type mice using an IMAC bead-binding assay and HFaq treatment. In Fig. 4*A*, Western blot analysis of wild-type tissues showed that α-DG in testis has a MW of 90,000 and was not recognized by the IIH6 antibody,

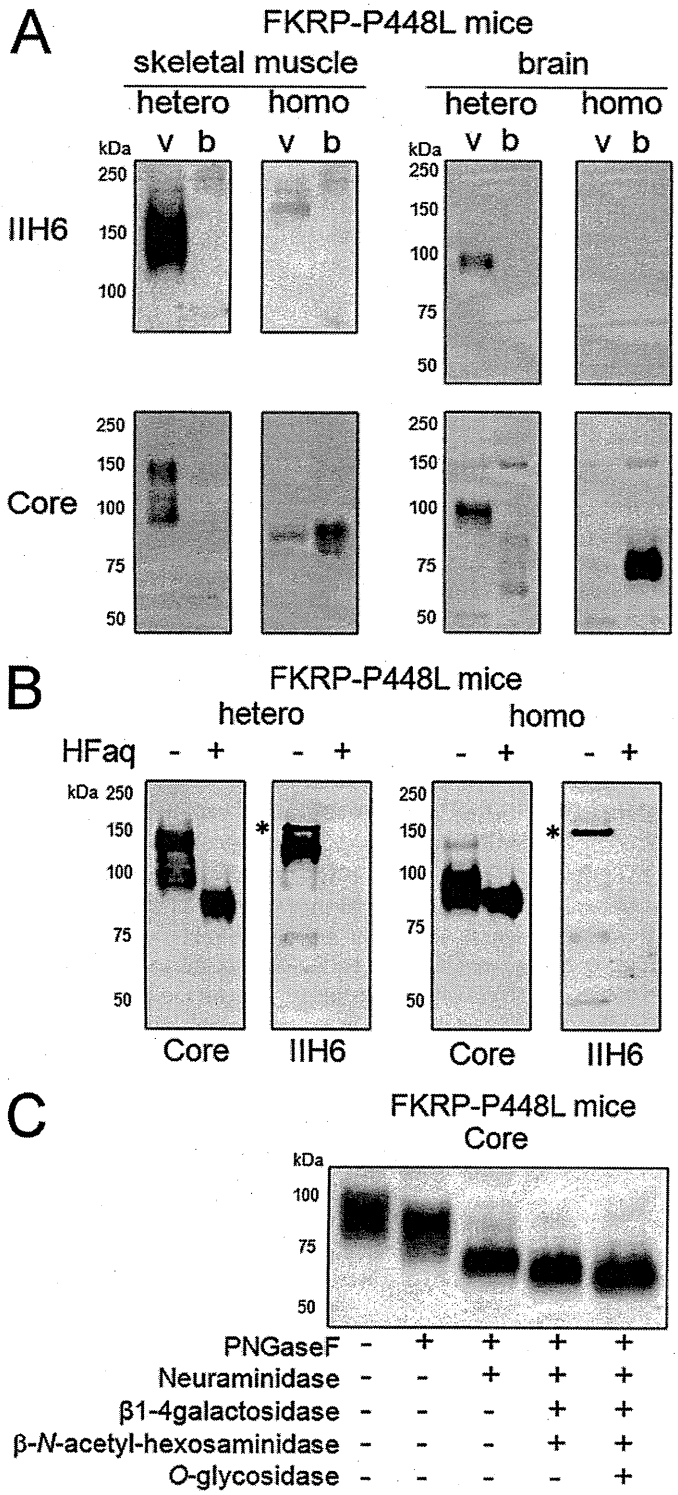

FIGURE 2. **Defects of post-phosphoryl modification in the *FKRP*-deficient disease model.** *A*, IMAC bead-binding assay for *FKRP*-deficient mice. α-DG enriched samples from skeletal muscle and brain of FKRP-P448L homozygous (*homo*) and litter control heterozygous (*hetero*) mice were tested for binding to IMAC beads. The void (v) and bound (b) fractions were collected. *B*, chemical dephosphorylation of α-DG from *FKRP*-deficient mice. α-DG enriched samples from skeletal muscle of FKRP-P448L homozygous (*homo*) and litter control heterozygous (*hetero*) mice were treated with HFaq. *, these bands are not likely derived from α-DG because they are not recognized by antibodies against the α-DG core protein. *C*, enzymatic deglycosylation of α-DG from *FKRP*-deficient mice. α-DG-enriched samples from skeletal muscle of FKRP-P448L homozygous mice were digested with glycosidase mixtures (peptide-*N*-glycosidase (*PNGase F*), neuraminidase, β1–4 galactosidase/β-*N*-acetyl-hexosaminidase, and *O*-glycosidase). Following the IMAC bead-binding assay, HFaq treatment, and enzymatic digestions, the samples were analyzed by Western blot, using antibodies against the α-DG core protein (*Core*) or the functionally glycosylated form (*IIH6*). *v*, void fraction; *b*, bound fraction.

and that lung α-DG consists of two major detectable populations (IIH6-positive > 100,000, minor form, *arrow*; IIH6-negative < 100,000, major form, *arrowhead*). Both testis and lung IIH6-negative α-DG were found to bind to IMAC beads, in contrast with IIH6-positive α-DG in skeletal muscle, brain, liver, and lung (Fig. 4*A*). Furthermore, HFaq treatment reduced the MW of α-DG to ~75,000 in wild-type skeletal muscle, brain, and liver. On the other hand, the MW shift observed in testis α-DG and IIH6-negative lung α-DG was relatively minor following HFaq treatment (Fig. 4*B*). These data indicate the absence of post-phosphoryl modification on α-DG in some wild-type tissues. Ligand overlay assays showed that IIH6-positive α-DGs in skeletal muscle, brain, and lung bound to the ligand proteins laminin α1, α2, and agrin, whereas IIH6-negative α-DG in testis and lung did not bind to these ligands (Fig. 5). Altogether, these data confirm that IIH6-reactivity and laminin-binding activity in α-DG are associated with post-phosphoryl modification.

Because lung and testis tissues contain heterogeneous cell types, we also examined the established cell lines CHL (lung epithelial cells derived from Chinese hamster) and TM3 (Leydig cells derived from mouse testis). Both CHL and TM3 cells showed detectable amounts of endogenous α-DG using the core antibody, but they did not react with IIH6 (Fig. 6, *A* and *D*). RT-PCR analysis showed that known genes (*Large*, *POMT1*, *POMT2*, *POMGnT1*, *fukutin*, *FKRP*, and *β3GnT1*) involved in α-DG glycosylation were expressed in TM3 cells (Fig. 6*B*). β3GnT1 has been reported to be required for laminin-binding glycan synthesis through formation of a complex with LARGE (31). We did not examine expression in CHL cells because the sequences of these genes have not yet been determined in the hamster. Endogenous α-DG in CHL and TM3 cells bound to IMAC beads (Fig. 6*A*). HFaq treatment resulted in almost no change in the MW of α-DG in both CHL and TM3 cells (Fig. 6*C*), as was similarly seen in lung and testis tissues (Fig. 4*B*). Following sequential digestion with glycosidases, α-DG in both CHL and TM3 cells showed stepwise reductions in MW (Fig. 6*D*). These data suggest that the post-phosphoryl modification is absent from IIH6-negative α-DG in CHL and TM3 cells.

DISCUSSION

In the present study, we demonstrate for the first time that FKRP is involved in post-phosphoryl modification on *O*-mannose of α-DG. We also show that even in wild type, α-DG in certain tissues such as lung and testis lacks the post-phosphoryl modification.

Abnormal glycosylation of α-DG in dystroglycanopathies is usually determined by a loss of reactivity against monoclonal antibodies VIA4–1 or IIH6. Mutations in the POMT1/POMT2 complex result in *O*-mannosylation defects (13–15); therefore, *O*-mannosyl phosphorylation does not occur. α-DG in cells with mutations in *Large*, *fukutin*, or *POMGnT1* does not undergo further modification from phospho-mannose residues

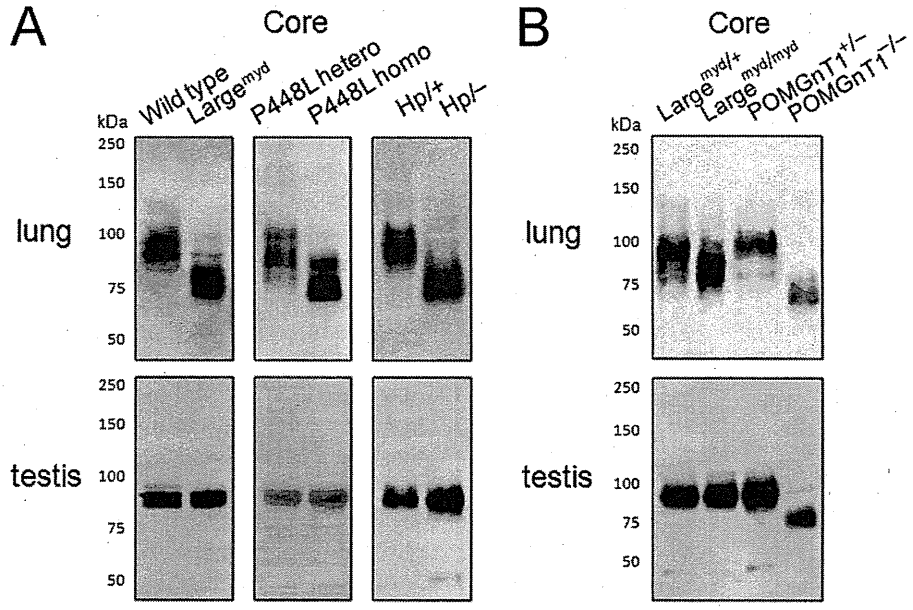

FIGURE 3. **α-DG in lung and testis from dystroglycanopathy models.** *A*, α-DG was enriched from lung and testis of wild-type, *Large*^{myd}, FKRP-P448L heterozygous or homozygous mice, and knock-in mice with a human retrotransposal allele and an intact mouse *fukutin* allele (Hp/+) or *fukutin*-deficient mice (Hp/−), and then analyzed by Western blot. *B*, the molecular weight of α-DGs from lung and testis of *POMGnT1*-deficient mice (*POMGnT1*$^{-/-}$) was compared with those of litter heterozygous mice (*POMGnT1*$^{+/-}$) and *Large*-deficient mice (*Large*$^{myd/myd}$).

(12). Our data add new evidence that mutations in *FKRP* also result in the absence of the post-phosphoryl moiety. It remains unclear how defects in *Large*, *fukutin*, *POMGnT1*, or *FKRP* all result in the same loss of the post-phosphoryl modification. A possible explanation is that these proteins may form a complex or be sequentially activated to create the post-phosphoryl moiety. POMGnT1 catalyzes GlcNAc transfer to *O*-mannose, and thus, it may not have direct involvement in the synthesis of the post-phosphoryl structure; however, the defects in post-phosphoryl modification in *POMGnT1*-deficient cells or tissues, shown here and in another study (12), indicate that the GlcNAc-β1,2 branch on *O*-mannose might provide favorable circumstances for the post-phosphoryl modification. Together, these studies have suggested that recognition by IIH6 requires at least the post-phosphoryl structure on *O*-mannose.

The range of α-DG molecular size and its reactivity to the monoclonal antibody IIH6 varies widely among different tissues. This has been thought to result from tissue-specific glycosylation on α-DG (1, 30). Our results indicate that post-phosphoryl modification is tissue-specific and thus suggest that the difference is largely determined by the extent and/or the proportion of post-phosphoryl modification. In light of the lack of post-phosphoryl modification in normal tissues such as lung and testis, even in the presence of transcripts of all known genes responsible for α-DG glycosylation, possible explanations are that they may not be properly translated; their protein products may be inactive (*e.g.* improper cellular location and lack of modification); or protein levels are not sufficient for α-DG glycosylation. Another possibility is that there could exist other yet-to-be identified mechanisms for α-DG modification, for example, a negative regulator, or novel genes. Supporting this idea, a large-scale genetic study has indicated that almost half of dystroglycanopathy cases can be explained by unidentified disease-causative genes or factors (32). Some of these cases might be caused by mutations in unidentified disease-causative genes, whose products are involved in post-phosphoryl modification, and such genes might not be expressed in wild-type tissues lacking post-phosphoryl modification of α-DG. This situation is exemplified in studies using cancer cells. It has been reported that several malignant cancer cell types lose the laminin-binding glycan of α-DG due to epigenetic down-regulation of *LARGE* or defects in the LARGE-binding protein β3GnT1, raising the possibility of defects in post-phosphoryl modification of α-DG in those cells (31, 33).

Reduction or loss of IIH6 reactivity can be rescued by forced expression of LARGE (34, 35). It has been shown that exogenously expressed LARGE can overcome defects in the laminin-binding activity of α-DG in *fukutin*- or *POMGnT1*-deficient cells or tissues (26, 34). On the other hand, if cells lack a gene that acts via direct interaction with LARGE, such as β3GnT1, forced expression of LARGE would fail to produce IIH6 reactivity (31). We observed that forced expression of LARGE could produce IIH6 reactivity in CHL cells, and newly produced IIH6-reactive α-DG no longer bound to IMAC-beads (supplemental Fig. 1). The effect of LARGE overexpression on α-DG glycosylation was also observed in TM3 cells. These data indicate that CHL and TM3 cells might lack gene activity that is involved in the post-phosphoryl modification, but such defects can be compensated by overexpression of LARGE.

Our results also raised a question about the function of the non-laminin-binding form of α-DG. It is generally thought that α-DG function relies on its glycosylation-dependent laminin-binding activity; on the other hand, several studies have suggested that dystroglycan possesses functions beyond that of a laminin receptor. The N-terminal domain of α-DG, which can be shed from the core protein into the extracellular space and body fluid (36), has been shown to promote neurite extension in PC 12 cells, suggesting that it has a biological function (37).

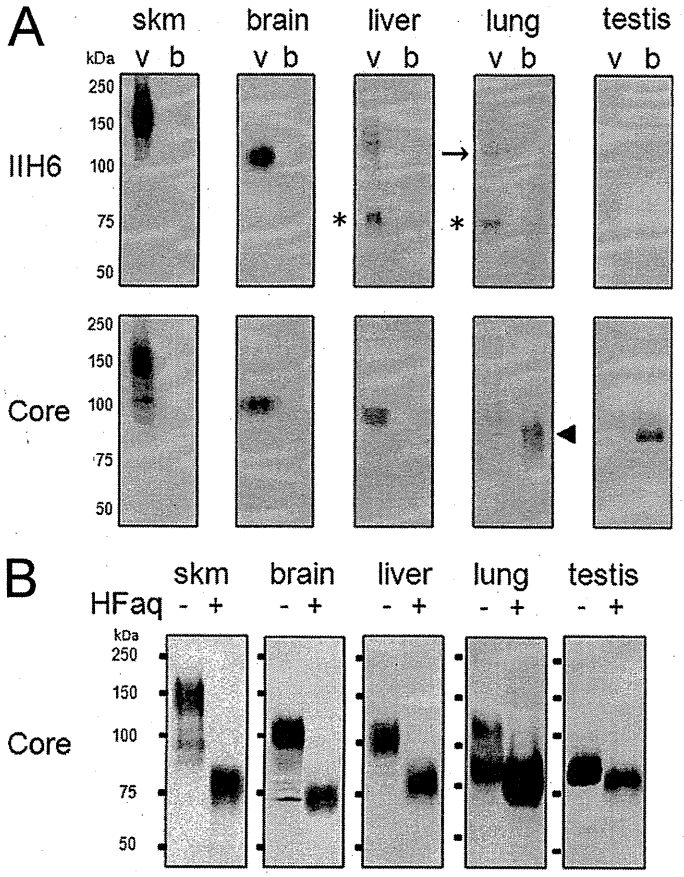

FIGURE 4. **Absence of post-phosphoryl modification in wild-type lung and testis.** *A*, IMAC bead-binding assays for α-DG from wild-type tissues. α-DG-enriched samples from skeletal muscle (*skm*), brain, liver, lung, and testis of C57BL/6 mice were tested for binding to IMAC beads. The void (*v*) and bound (*b*) fractions were collected. The *arrow* indicates the IIH6-positive population of lung α-DG. The *arrowhead* indicates the IIH6-negative fraction of lung α-DG bound to beads. An *asterisk* indicates a background signal that is not specific for IIH6 antibody. *B*, chemical dephosphorylation of α-DG from wild-type tissues. α-DG-enriched samples from skeletal muscle (*skm*), brain, liver, lung and testis of C57BL/6 mice were treated with HFaq and then analyzed by Western blot using anti-DG core antibody.

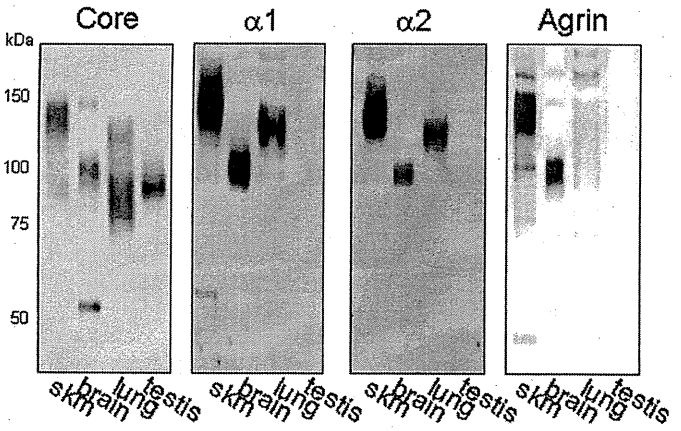

FIGURE 5. **Ligand-binding assays for lung and testis α-DG.** Ligand binding (laminin α1, α2, and agrin) was assessed in α-DG-enriched samples from skeletal muscle (*skm*), brain, lung, and testis using ligand overlay assays.

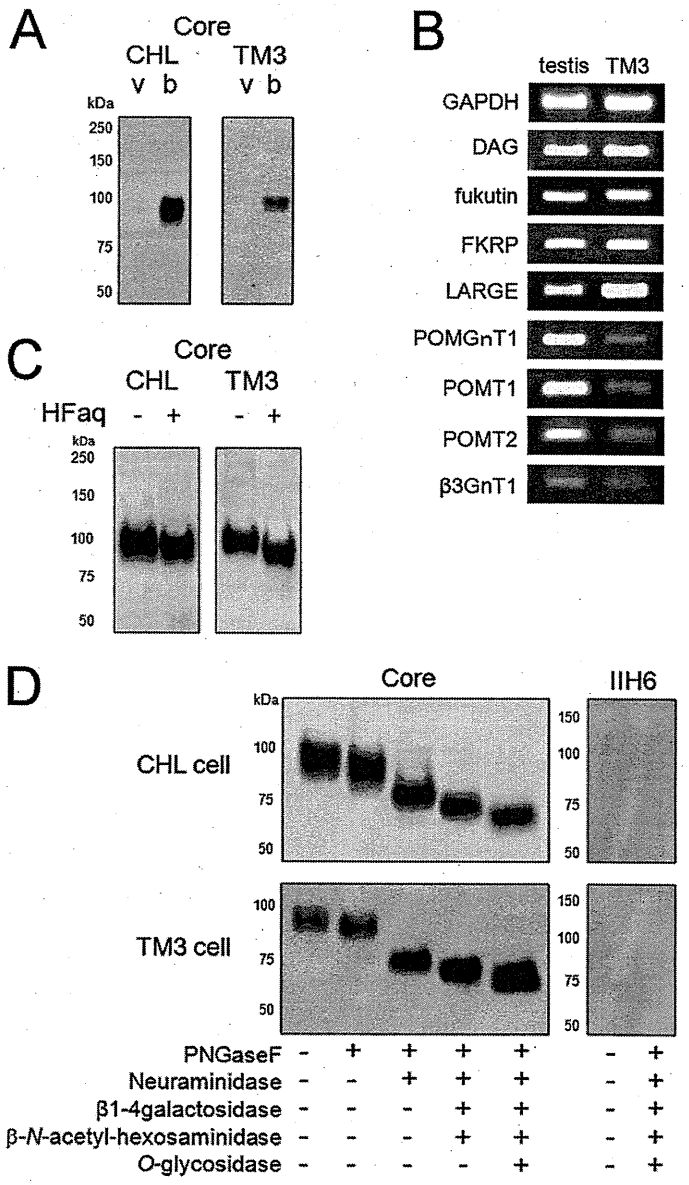

FIGURE 6. **Absence of post-phosphoryl modification of α-DG in CHL and TM3 cells.** *A*, IMAC bead-binding assays for α-DG from CHL cells and TM3 cells. α-DG-enriched samples from CHL and TM3 cell lysates were tested for binding to IMAC beads. The void (*v*) and bound (*b*) fractions were collected. *B*, RT-PCR analysis of TM3 cells. RT-PCR analysis was performed to detect transcripts encoding proteins implicated in α-DG glycosylation. *C*, chemical dephosphorylation of α-DG from wild-type tissues. α-DG-enriched samples from CHL and TM3 cell lysates were treated with HFaq. *D*, enzymatic deglycosylation of α-DG from CHL and TM3 cells. α-DG-enriched samples from CHL and TM3 cells were digested with glycosidase mixtures (peptide-*N*-glycosidase (*PNGaseF*), neuraminidase, β1–4 galactosidase/β-*N*-acetyl-hexosaminidase, and *O*-glycosidase). Following the IMAC bead-binding assay, HFaq treatment, and enzymatic deglycosylation, the samples were analyzed by Western blot, using antibodies against the α-DG core protein (Core) or the functionally glycosylated form (IIH6).

α-DG might have ligand proteins that do not require *O*-mannosyl modification; for example, a chondroitin sulfate proteoglycan biglycan has been shown to interact with protein core of the α-DG C-terminal domain in a glycosylation-independent manner (38). DG is also thought to serve as a signaling molecule (39). For example, the cytoplasmic tail of β-DG interacts with several signaling molecules, including caveolin-3, Grb2, and mitogen-activated protein (MAP) kinase kinase 2 (40). Although the significance of these interactions is not well understood, it is possible that DG serves as a scaffold to position interacting proteins at their proper cellular location (9, 41). Taken together, these observations suggest that the presence of

DG without post-phosphoryl modification could be functionally important in various tissue types.

Future work to determine the molecular structure of the post-phosphoryl moiety, and to identify genes involved in its biosynthesis, will contribute to understanding the biological basis of this unique post-translational modification and disease pathogenesis. Our present data contributes to the foundation for such research. Recently, it has been shown that LARGE can act as a bifunctional glycosyltransferase, with both xylosyltransferase and glucuronyltransferase activities (42). Involvement of these activities in the post-phosphoryl modification also should be clarified in the future.

Overall, our results indicate that phosphorylated *O*-mannose not only plays critical roles in the pathogenesis of dystroglycanopathy but also is a key determinant in the maturation of α-DG as a laminin receptor in normal tissues and cells.

Acknowledgments—We thank Chiyomi Ito and Elizabeth Keramaris for technical support. We also thank Dr. Yuko Miyagoe-Suzuki and Dr. Shin'ichi Takeda for providing POMGnT1 knock-out mice and Dr. Jennifer Logan for help in editing the manuscript.

REFERENCES

1. Barresi, R., and Campbell, K. P. (2006) Dystroglycan: From biosynthesis to pathogenesis of human disease. *J. Cell Sci.* **119,** 199–207
2. Ibraghimov-Beskrovnaya, O., Ervasti, J. M., Leveille, C. J., Slaughter, C. A., Sernett, S. W., and Campbell, K. P. (1992) Primary structure of dystrophin-associated glycoproteins linking dystrophin to the extracellular matrix. *Nature* **355,** 696–702
3. Gee, S. H., Montanaro, F., Lindenbaum, M. H., and Carbonetto, S. (1994) Dystroglycan-α, a dystrophin-associated glycoprotein, is a functional agrin receptor. *Cell* **77,** 675–686
4. Bowe, M. A., Deyst, K. A., Leszyk, J. D., and Fallon, J. R. (1994) Identification and purification of an agrin receptor from Torpedo postsynaptic membranes: A heteromeric complex related to the dystroglycans. *Neuron* **12,** 1173–1180
5. Talts, J. F., Andac, Z., Göhring, W., Brancaccio, A., and Timpl, R. (1999) Binding of the G domains of laminin α1 and α2 chains and perlecan to heparin, sulfatides, α-dystroglycan, and several extracellular matrix proteins. *EMBO J.* **18,** 863–870
6. Sugita, S., Saito, F., Tang, J., Satz, J., Campbell, K., and Südhof, T. C. (2001) A stoichiometric complex of neurexins and dystroglycan in brain. *J. Cell Biol.* **154,** 435–445
7. Sato, S., Omori, Y., Katoh, K., Kondo, M., Kanagawa, M., Miyata, K., Funabiki, K., Koyasu, T., Kajimura, N., Miyoshi, T., Sawai, H., Kobayashi, K., Tani, A., Toda, T., Usukura, J., Tano, Y., Fujikado, T., and Furukawa, T. (2008) Pikachurin, a dystroglycan ligand, is essential for photoreceptor ribbon synapse formation. *Nat. Neurosci.* **11,** 923–931
8. Godfrey, C., Foley, A. R., Clement, E., and Muntoni, F. (2011) Dystroglycanopathies: Coming into focus. *Curr. Opin. Genet. Dev.* **21,** 278–285
9. Michele, D. E., and Campbell, K. P. (2003) Dystrophin-glycoprotein complex: Post-translational processing and dystroglycan function. *J. Biol. Chem.* **278,** 15457–15460
10. Toda, T., Kobayashi, K., Takeda, S., Sasaki, J., Kurahashi, H., Kano, H., Tachikawa, M., Wang, F., Nagai, Y., Taniguchi, K., Taniguchi, M., Sunada, Y., Terashima, T., Endo, T., and Matsumura, K. (2003) Fukuyama-type congenital muscular dystrophy (FCMD) and alpha-dystroglycanopathy. *Congenit. Anom.* **43,** 97–104
11. Chiba, A., Matsumura, K., Yamada, H., Inazu, T., Shimizu, T., Kusunoki, S., Kanazawa, I., Kobata, A., and Endo, T. (1997) Structures of sialylated *O*-linked oligosaccharides of bovine peripheral nerve α-dystroglycan. The role of a novel *O*-mannosyl-type oligosaccharide in the binding of α-dystroglycan with laminin. *J. Biol. Chem.* **272,** 2156–2162
12. Yoshida-Moriguchi, T., Yu, L., Stalnaker, S. H., Davis, S., Kunz, S., Madson, M., Oldstone, M. B., Schachter, H., Wells, L., and Campbell, K. P. (2010) *O*-mannosyl phosphorylation of α-dystroglycan is required for laminin binding. *Science* **327,** 88–92
13. Manya, H., Chiba, A., Yoshida, A., Wang, X., Chiba, Y., Jigami, Y., Margolis, R. U., and Endo, T. (2004) Demonstration of mammalian protein *O*-mannosyltransferase activity: Coexpression of POMT1 and POMT2 required for enzymatic activity. *Proc. Natl. Acad. Sci. U.S.A.* **101,** 500–505
14. Beltrán-Valero de Bernabé, D., Currier, S., Steinbrecher, A., Celli, J., van Beusekom, E., van der Zwaag, B., Kayserili, H., Merlini, L., Chitayat, D., Dobyns, W. B., Cormand, B., Lehesjoki, A. E., Cruces, J., Voit, T., Walsh, C. A., van Bokhoven, H., and Brunner, H. G. (2002) Mutations in the *O*-mannosyltransferase gene POMT1 give rise to the severe neuronal migration disorder Walker-Warburg syndrome. *Am. J. Hum. Genet.* **71,** 1033–1043
15. van Reeuwijk, J., Janssen, M., van den Elzen, C., Beltran-Valero de Bernabé, D., Sabatelli, P., Merlini, L., Boon, M., Scheffer, H., Brockington, M., Muntoni, F., Huynen, M. A., Verrips, A., Walsh, C. A., Barth, P. G., Brunner, H. G., and van Bokhoven, H. (2005) POMT2 mutations cause α-dystroglycan hypoglycosylation and Walker-Warburg syndrome. *J. Med. Genet.* **42,** 907–912
16. Yoshida, A., Kobayashi, K., Manya, H., Taniguchi, K., Kano, H., Mizuno, M., Inazu, T., Mitsuhashi, H., Takahashi, S., Takeuchi, M., Herrmann, R., Straub, V., Talim, B., Voit, T., Topaloglu, H., Toda, T., and Endo, T. (2001) Muscular dystrophy and neuronal migration disorder caused by mutations in a glycosyltransferase, POMGnT1. *Dev. Cell* **1,** 717–724
17. Michele, D. E., Barresi, R., Kanagawa, M., Saito, F., Cohn, R. D., Satz, J. S., Dollar, J., Nishino, I., Kelley, R. I., Somer, H., Straub, V., Mathews, K. D., Moore, S. A., and Campbell, K. P. (2002) Post-translational disruption of dystroglycan-ligand interactions in congenital muscular dystrophies. *Nature* **418,** 417–422
18. Combs, A. C., and Ervasti, J. M. (2005) Enhanced laminin binding by α-dystroglycan after enzymatic deglycosylation. *Biochem. J.* **390,** 303–309
19. Kobayashi, K., Nakahori, Y., Miyake, M., Matsumura, K., Kondo-Iida, E., Nomura, Y., Segawa, M., Yoshioka, M., Saito, K., Osawa, M., Hamano, K., Sakakihara, Y., Nonaka, I., Nakagome, Y., Kanazawa, I., Nakamura, Y., Tokunaga, K., and Toda, T. (1998) An ancient retrotransposal insertion causes Fukuyama-type congenital muscular dystrophy. *Nature* **394,** 388–392
20. Brockington, M., Blake, D. J., Prandini, P., Brown, S. C., Torelli, S., Benson, M. A., Ponting, C. P., Estournet, B., Romero, N. B., Mercuri, E., Voit, T., Sewry, C. A., Guicheney, P., and Muntoni, F. (2001) Mutations in the *fukutin*-related protein gene (FKRP) cause a form of congenital muscular dystrophy with secondary laminin α2 deficiency and abnormal glycosylation of α-dystroglycan. *Am. J. Hum. Genet.* **69,** 1198–1209
21. Brockington, M., Yuva, Y., Prandini, P., Brown, S. C., Torelli, S., Benson, M. A., Herrmann, R., Anderson, L. V., Bashir, R., Burgunder, J. M., Fallet, S., Romero, N., Fardeau, M., Straub, V., Storey, G., Pollitt, C., Richard, I., Sewry, C. A., Bushby, K., Voit, T., Blake, D. J., and Muntoni, F. (2001) Mutations in the fukutin-related protein gene (FKRP) identify limb girdle muscular dystrophy 2I as a milder allelic variant of congenital muscular dystrophy MDC1C. *Hum. Mol. Genet.* **10,** 2851–2859
22. Grewal, P. K., Holzfeind, P. J., Bittner, R. E., and Hewitt, J. E. (2001) Mutant glycosyltransferase and altered glycosylation of α-dystroglycan in the myodystrophy mouse. *Nat. Genet.* **28,** 151–154
23. Longman, C., Brockington, M., Torelli, S., Jimenez-Mallebrera, C., Kennedy, C., Khalil, N., Feng, L., Saran, R. K., Voit, T., Merlini, L., Sewry, C. A., Brown, S. C., and Muntoni, F. (2003) Mutations in the human LARGE gene cause MDC1D, a novel form of congenital muscular dystrophy with severe mental retardation and abnormal glycosylation of α-dystroglycan. *Hum. Mol. Genet.* **12,** 2853–2861
24. Xiong, H., Kobayashi, K., Tachikawa, M., Manya, H., Takeda, S., Chiyonobu, T., Fujikake, N., Wang, F., Nishimoto, A., Morris, G. E., Nagai, Y., Kanagawa, M., Endo, T., and Toda, T. (2006) Molecular interaction between fukutin and POMGnT1 in the glycosylation pathway of α-dystroglycan. *Biochem. Biophys. Res. Commun.* **350,** 935–941
25. Chan, Y. M., Keramaris-Vrantsis, E., Lidov, H. G., Norton, J. H., Zinchenko, N., Gruber, H. E., Thresher, R., Blake, D. J., Ashar, J., Rosen-

feld, J., and Lu, Q. L. (2010) Fukutin-related protein is essential for mouse muscle, brain, and eye development and mutation recapitulates the wide clinical spectrums of dystroglycanopathies. *Hum. Mol. Genet.* **19,** 3995–4006
26. Kanagawa, M., Nishimoto, A., Chiyonobu, T., Takeda, S., Miyagoe-Suzuki, Y., Wang, F., Fujikake, N., Taniguchi, M., Lu, Z., Tachikawa, M., Nagai, Y., Tashiro, F., Miyazaki, J., Tajima, Y., Takeda, S., Endo, T., Kobayashi, K., Campbell, K. P., and Toda, T. (2009) Residual laminin-binding activity and enhanced dystroglycan glycosylation by LARGE in novel model mice to dystroglycanopathy. *Hum. Mol. Genet.* **18,** 621–631
27. Miyagoe-Suzuki, Y., Masubuchi, N., Miyamoto, K., Wada, M. R., Yuasa, S., Saito, F., Matsumura, K., Kanesaki, H., Kudo, A., Manya, H., Endo, T., and Takeda, S. (2009) Reduced proliferative activity of primary POMGnT1-null myoblasts *in vitro*. *Mech. Dev.* **126,** 107–116
28. Hozumi, K., Suzuki, N., Uchiyama, Y., Katagiri, F., Kikkawa, Y., and Nomizu, M. (2009) Chain-specific heparin-binding sequences in the laminin α chain LG45 modules. *Biochemistry* **48,** 5375–5381
29. Manya, H., Bouchet, C., Yanagisawa, A., Vuillaumier-Barrot, S., Quijano-Roy, S., Suzuki, Y., Maugenre, S., Richard, P., Inazu, T., Merlini, L., Romero, N. B., Leturcq, F., Bezier, I., Topaloglu, H., Estournet, B., Seta, N., Endo, T., and Guicheney, P. (2008) Protein *O*-mannosyltransferase activities in lymphoblasts from patients with α-dystroglycanopathies. *Neuromuscul. Disord.* **18,** 45–51
30. Michele, D. E., Kabaeva, Z., Davis, S. L., Weiss, R. M., and Campbell, K. P. (2009) Dystroglycan matrix receptor function in cardiac myocytes is important for limiting activity-induced myocardial damage. *Circ. Res.* **105,** 984–993
31. Bao, X., Kobayashi, M., Hatakeyama, S., Angata, K., Gullberg, D., Nakayama, J., Fukuda, M. N., and Fukuda, M. (2009) Tumor suppressor function of laminin-binding α-dystroglycan requires a distinct β3-*N*-acetylglucosaminyltransferase. *Proc. Natl. Acad. Sci. U.S.A.* **106,** 12109–12114
32. Godfrey, C., Clement, E., Mein, R., Brockington, M., Smith, J., Talim, B., Straub, V., Robb, S., Quinlivan, R., Feng, L., Jimenez-Mallebrera, C., Mercuri, E., Manzur, A. Y., Kinali, M., Torelli, S., Brown, S. C., Sewry, C. A., Bushby, K., Topaloglu, H., North, K., Abbs, S., and Muntoni, F. (2007) Refining genotype phenotype correlations in muscular dystrophies with defective glycosylation of dystroglycan. *Brain* **130,** 2725–2735
33. de Bernabé, D. B., Inamori, K., Yoshida-Moriguchi, T., Weydert, C. J., Harper, H. A., Willer, T., Henry, M. D., and Campbell, K. P. (2009) Loss of α-dystroglycan laminin binding in epithelium-derived cancers is caused by silencing of LARGE. *J. Biol. Chem.* **284,** 11279–11284
34. Barresi, R., Michele, D. E., Kanagawa, M., Harper, H. A., Dovico, S. A., Satz, J. S., Moore, S. A., Zhang, W., Schachter, H., Dumanski, J. P., Cohn, R. D., Nishino, I., and Campbell, K. P. (2004) LARGE can functionally bypass α-dystroglycan glycosylation defects in distinct congenital muscular dystrophies. *Nat. Med.* **10,** 696–703
35. Patnaik, S. K., and Stanley, P. (2005) Mouse large can modify complex *N*- and mucin *O*-glycans on α-dystroglycan to induce laminin binding. *J. Biol. Chem.* **280,** 20851–20859
36. Saito, F., Saito-Arai, Y., Nakamura, A., Shimizu, T., and Matsumura, K. (2008) Processing and secretion of the N-terminal domain of α-dystroglycan in cell culture media. *FEBS Lett.* **582,** 439–444
37. Hall, H., Bozic, D., Michel, K., and Hubbell, J. A. (2003) N-terminal α-dystroglycan binds to different extracellular matrix molecules expressed in regenerating peripheral nerves in a protein-mediated manner and promotes neurite extension of PC12 cells. *Mol. Cell Neurosci.* **24,** 1062–1073
38. Bowe, M. A., Mendis, D. B., and Fallon, J. R. (2000) The small leucine-rich repeat proteoglycan biglycan binds to α-dystroglycan and is up-regulated in dystrophic muscle. *J. Cell Biol.* **148,** 801–810
39. Higginson, J. R., and Winder, S. J. (2005) Dystroglycan: A multifunctional adaptor protein. *Biochem. Soc. Trans.* **33,** 1254–1255
40. Spence, H. J., Dhillon, A. S., James, M., and Winder, S. J. (2004) Dystroglycan, a scaffold for the ERK-MAP kinase cascade. *EMBO Rep.* **5,** 484–489
41. Moore, C. J., and Winder, S. J. (2010) Dystroglycan versatility in cell adhesion: A tale of multiple motifs. *Cell Commun. Signal.* **8,** 3
42. Inamori, K., Yoshida-Moriguchi, T., Hara, Y., Anderson, M. E., Yu, L., Campbell, K. P. (2012) Dystroglycan function requires xylosyl- and glucuronyltransferase activities of LARGE. *Science* **335,** 93–96

THE JOURNAL OF BIOLOGICAL CHEMISTRY VOL. 287, NO. 11, pp. 8398–8406, March 9, 2012

Mislocalization of Fukutin Protein by Disease-causing Missense Mutations Can Be Rescued with Treatments Directed at Folding Amelioration*[S]

Received for publication, September 6, 2011, and in revised form, January 16, 2012 Published, JBC Papers in Press, January 24, 2012, DOI 10.1074/jbc.M111.300905

Masaji Tachikawa, Motoi Kanagawa, Chih-Chieh Yu, Kazuhiro Kobayashi, and Tatsushi Toda[1]

From the Division of Neurology/Molecular Brain Science, Kobe University Graduate School of Medicine, Kobe 650-0017, Japan

Background: The molecular pathogenesis of fukutin-deficient dystroglycanopathy remains unclear, and no effective treatment is available.
Results: Some disease-causing missense fukutin mutants showed mislocalization in cultured cells, which can be corrected by treatments directed at folding amelioration.
Conclusion: Correction of cellular localization of disease-causing mutants may have a therapeutic benefit.
Significance: A possible therapeutic strategy for fukutin-deficient dystroglycanopathy is proposed based on its molecular pathogenesis.

Fukuyama-type congenital muscular dystrophy (FCMD), the second most common childhood muscular dystrophy in Japan, is caused by alterations in the *fukutin* gene. Mutations in *fukutin* cause abnormal glycosylation of α-dystroglycan, a cell surface laminin receptor; however, the exact function and pathophysiological role of fukutin are unclear. Although the most prevalent mutation in Japan is a founder retrotransposal insertion, point mutations leading to abnormal glycosylation of α-dystroglycan have been reported, both in Japan and elsewhere. To understand better the molecular pathogenesis of fukutin-deficient muscular dystrophies, we constructed 13 disease-causing missense *fukutin* mutations and examined their pathological impact on cellular localization and α-dystroglycan glycosylation. When expressed in C2C12 myoblast cells, wild-type fukutin localizes to the Golgi apparatus, whereas the missense mutants A170E, H172R, H186R, and Y371C instead accumulated in the endoplasmic reticulum. Protein *O*-mannose β1,2-*N*-acetylglucosaminyltransferase 1 (POMGnT1) also mislocalizes when co-expressed with these missense mutants. The results of nocodazole and brefeldin A experiments suggested that these mutant proteins were not transported to the Golgi via the anterograde pathway. Furthermore, we found that low temperature culture or curcumin treatment corrected the subcellular location of these missense mutants. Expression studies using *fukutin*-null mouse embryonic stem cells showed that the activity responsible for generating the laminin-binding glycan of α-dystroglycan was retained in these mutants. Together, our results suggest that some disease-causing missense mutations cause abnormal folding and localization of fukutin protein, and therefore we propose that folding amelioration directed at correcting the cellular localization may provide a therapeutic benefit to glycosylation-deficient muscular dystrophies.

Fukuyama-type congenital muscular dystrophy (FCMD,[2] MIM 253800) is the second most common childhood muscular dystrophy and one of the most prevalent autosomal recessive disorders in the Japanese population. FCMD is clinically characterized by congenital muscular dystrophy in combination with cortical dysgenesis (micropolygyria) and ocular abnormalities (1). We identified *fukutin*, the gene responsible for FCMD, on chromosome 9q31 by linkage analysis and positional cloning (2, 3). Most FCMD-bearing chromosomes have been derived from a single ancestral founder and have a 3-kb retrotransposal insertion in the 3′ noncoding region of the *fukutin* gene. Compound heterozygosity, with both a retrotransposal mutation and a point mutation in *fukutin*, is sometimes seen and generally exhibits more severe pathologies (4, 5). However, a recent report has identified several Japanese patients presenting with mild limb-girdle dystrophy (LGMD2M, MIM 611588) and normal intelligence (6) and who have a retrotransposal mutation and a point mutation in the *fukutin* gene. Outside Japan, *fukutin* mutations have been reported in patients with various phenotypes, from Walker-Warburg syndrome (WWS, MIM 236670) to LGMD (7–13). Overall, the current common understanding is that *fukutin* alterations can give rise to a wide spectrum of phenotypes.

Mutations in *fukutin* cause abnormal glycosylation of the cell surface laminin receptor α-dystroglycan (DG) and reduce its

* This work was supported by the Ministry of Health, Labor, and Welfare of Japan Intramural Research Grant for Neurological and Psychiatric Disorders of National Center of Neurology and Psychiatry 23B-5 and Research on Psychiatric and Neurological Diseases and Mental Health (H20-016), Ministry of Education, Culture, Sports, Science, and Technology of Japan Grant-in-aid for Scientific Research (A) 23249049 (to T. T.), Japan Society for the Promotion of Science Grant-in-aid for Young Scientists (B) 18790220 (to M. T.), Takeda Science Foundation (to M. K.), and Global COE (Centers of Excellence) Program Frontier Biomedical Science Underlying Organelle Network Biology.
[S] This article contains supplemental Tables I–III, Experimental Procedures, and Figs. 1–3.
[1] To whom correspondence should be addressed. Tel.: 81-78-382-6286; Fax: 81-78-382-6288; E-mail: toda@med.kobe-u.ac.jp.

[2] The abbreviations used are: FCMD, Fukuyama-type congenital muscular dystrophy; BFA, brefeldin A; DG, dystroglycan; ER, endoplasmic reticulum; FKRP, fukutin-related protein; LGMD, limb-girdle muscular dystrophy; POMGnT1, protein *O*-mannose β1,2-*N*-acetylglucosaminyltransferase 1; POMT1, protein *O*-mannosyltransferase 1; POMT2, protein *O*-mannosyltransferase 2; WWS, Walker-Warburg syndrome.

laminin binding activity (14). The α- and β-DG complex is believed to provide physical strength to the sarcolemma by connecting the basal lamina to the cytoskeleton. Thus, abnormal glycosylation caused by *fukutin* mutations underlies FCMD molecular pathogenesis, but the exact function of fukutin remains unclear. The *fukutin* gene encodes a 461-amino acid protein with a predicted molecular mass of 53.7 kDa (3). Although endogenous fukutin protein has not been detected in cells, likely due to its low abundance, expression studies have proposed that *fukutin* gene product localizes to the Golgi apparatus (15, 16). Fukutin protein contains a transmembrane domain (3, 16), a putative *N*-glycosylation site (3), and a DxD motif that is predicted to modify cell surface glycoproteins or glycolipids (17). Previously, we showed that the transmembrane domain of fukutin binds to the protein *O*-mannose β1,2-*N*-acetylglucosaminyltransferase 1 (POMGnT1), which is encoded by the responsible gene for muscle-eye-brain disease (MIM 253280) (18), suggesting that fukutin affects the enzymatic activity of POMGnT1 (16). Other regions of the fukutin protein share no sequence homology with known proteins. In addition to FCMD, several other forms of muscular dystrophy are caused by abnormal glycosylation of α-DG; together, these conditions are termed as "dystroglycanopathy." To date, six genes (protein *O*-mannosyltransferase 1 (*POMT1*), protein *O*-mannosyltransferase 2 (*POMT2*), *POMGnT1*, *fukutin*, fukutin-related protein (*FKRP*), and *LARGE*) have been implicated in dystroglycanopathies, and all are thought to be involved in glycosylation of α-DG (19–23). POMGnT1 and the POMT1/2 complex are known to have glycosyltransferase activities directly involved in synthesis of *O*-mannosyl sugar chains on α-DG (18, 24). Quite recently, it has been shown that LARGE can act as a bifunctional glycosyltransferase with both xylosyltransferase and glucuronyltransferase activities (25). On the other hand, the exact function of FKRP is unknown. Yoshida-Moriguchi *et al.* reported that a phosphodiester-linked moiety on *O*-mannose of α-DG is defective in LARGE- or fukutin-deficient dystroglycanopathies (26). This finding suggests that LARGE and fukutin might be involved in the synthesis of the postphosphoryl modification, which is necessary for laminin binding activity.

The precise pathogenic mechanism of FCMD has remained obscure. In this report, to understand molecular pathogenesis of fukutin-deficient muscular dystrophies, we constructed 13 disease-causing missense *fukutin* mutations that have been reported inside and outside Japan (4–6, 9–13, 27, 28) and investigated their pathological roles in fukutin intracellular location. Four mutants (A170E, H172R, H186R, and Y371C) lost their Golgi localization and instead accumulated in the endoplasmic reticulum (ER) when expressed in C2C12 cultured cells. Using *fukutin*-null mouse embryonic stem (ES) cells, we showed that these mutants retain the activity responsible for α-DG glycosylation. Finally, we found that low temperature culture and curcumin treatment are effective in correcting the localization of these missense fukutin mutants.

EXPERIMENTAL PROCEDURES

Reagents—Brefeldin A (BFA) and nocodazole were obtained from Santa Cruz Biotechnology (Santa Cruz, CA). Curcumin was purchased from Nacalai Tesque (Kyoto, Japan).

Antibodies used in this study were as follows: monoclonal anti-V5 (Invitrogen), rabbit polyclonal anti-FLAG (Sigma), monoclonal anti-α-DG clone IIH6C4 (Millipore), monoclonal anti-β-DG clone 8D5 (Novocastra Laboratories, Newcastle, UK), monoclonal anti-GM130 (BD Biosciences), monoclonal anti-KDEL antibodies (Stressgen, Victoria, Canada); rabbit polyclonal anti-laminin (Sigma); and goat polyclonal antibody against the C-terminal region of α-DG (AP-074G-C) (29)

Vector Constructions and Site-directed Mutagenesis—For the construction of expression vectors, the coding regions of human *POMGnT1*, human *fukutin*, or human *FKRP* with a FLAG or a V5 epitope at the C terminus were cloned into the pEF1/V5-HisA vector (Invitrogen). Expression vectors encoding 13 different disease-causative missense fukutin mutants were constructed using site-directed mutagenesis. Mutations were confirmed by DNA sequencing.

Cell Culture, Transfection, and Immunofluorescence Detection—Mouse myoblast C2C12 cells were cultured in Dulbecco's modified Eagle Medium (DMEM) (Wako Pure Chemical Industries, Osaka, Japan) supplemented with 10% heat-inactivated fetal bovine serum (Invitrogen) and streptomycin (100 μg/ml) (Wako). Mouse ES cells were grown in DMEM with 15% heat-inactivated fetal bovine serum, 100 μM 2-mercaptoethanol, and streptomycin. Targeted disruptions of the *fukutin* gene in ES cells have been described previously (30).

Cell transfection was performed using Effectene (Qiagen) according to the manufacturer's protocol. 48 h after transfection, the cells were fixed with 4% paraformaldehyde in phosphate-buffered saline (PBS) and then permeabilized in PBS with 0.5% Triton X-100 (Nacalai Tesque). For immunofluorescence detection, after blocking with 1% BSA (Wako) in PBS at room temperature for 1 h, the cells were first incubated for 90 min with polyclonal anti-FLAG, monoclonal anti-GM130, monoclonal anti-KDEL, or monoclonal anti-V5 antibodies, followed by Alexa Fluor 488-conjugated anti-rabbit IgG and/or Alexa Fluor 546-conjugated anti-mouse IgG (Invitrogen) for 1 h at room temperature. After a final rinse with PBS, cells were observed by fluorescence microscopy using a Leica DMR microscope (Leica Microsystems, Wetzlar, Germany).

For BFA, nocodazole, or curcumin treatment, the cells were incubated with 5 μg/ml BFA or 10 μg/ml nocodazole for 2 h after 48 h of transfection, or 10 μg/ml curcumin for 24 h after 24 h of transfection. For statistical analysis of fukutin cellular localization, cells expressing fukutin were classified into four classes (Golgi localization, Golgi and around localization, dot localization, and ER localization) (see Fig. 6*A*). For statistical analysis of POMGnT1 localization, cells co-expressing fukutin/POMGnT1 were classified into three classes (Golgi localization with fukutin, Golgi localization without fukutin, and ER localization). The number of cells in each class was counted and analyzed using the χ^2 test.

Dystroglycan Preparation—DG was enriched from solubilized mouse ES cells. The ES cells were solubilized in 1 ml of PBS containing 1% Triton X-100 and protease inhibitor mixture (Nacalai Tesque). Solubilized fractions were incubated with 30 μl of wheat germ agglutinin-agarose beads (Vector Laboratories) at 4 °C for 2 h. The beads were washed five times with 1 ml of PBS containing 0.1% Triton X-100 and protease inhibitor